



TECH BRIEFS

NATIONAL AERONAUTICS AND SPACE ADMINISTRATION

-  **Technology Focus**
-  **Electronics/Computers**
-  **Software**
-  **Materials**
-  **Mechanics/Machinery**
-  **Manufacturing**
-  **Bio-Medical**
-  **Physical Sciences**
-  **Information Sciences**
-  **Books and Reports**

INTRODUCTION

Tech Briefs are short announcements of innovations originating from research and development activities of the National Aeronautics and Space Administration. They emphasize information considered likely to be transferable across industrial, regional, or disciplinary lines and are issued to encourage commercial application.

Additional Information on NASA Tech Briefs and TSPs

Additional information announced herein may be obtained from the NASA Technical Reports Server: <http://ntrs.nasa.gov>.

Please reference the control numbers appearing at the end of each Tech Brief. Information on NASA's Innovative Partnerships Program (IPP), its documents, and services is available on the World Wide Web at <http://www.ipp.nasa.gov>.

Innovative Partnerships Offices are located at NASA field centers to provide technology-transfer access to industrial users. Inquiries can be made by contacting NASA field centers listed below.

NASA Field Centers and Program Offices

Ames Research Center

David Morse
(650) 604-4724
david.r.morse@nasa.gov

Dryden Flight Research Center

Ron Young
(661) 276-3741
ronald.m.young@nasa.gov

Glenn Research Center

Kimberly A. Dalgleish-Miller
(216) 433-8047
kimberly.a.dalgleish@nasa.gov

Goddard Space Flight Center

Nona Cheeks
(301) 286-5810
nona.k.cheeks@nasa.gov

Jet Propulsion Laboratory

Dan Broderick
(818) 354-1314
daniel.f.broderick@jpl.nasa.gov

Johnson Space Center

John E. James
(281) 483-3809
john.e.james@nasa.gov

Kennedy Space Center

David R. Makufka
(321) 867-6227
david.r.makufka@nasa.gov

Langley Research Center

Michelle Ferebee
(757) 864-5617
michelle.t.ferebee@nasa.gov

Marshall Space Flight Center

Terry L. Taylor
(256) 544-5916
terry.taylor@nasa.gov

Stennis Space Center

Ramona Travis
(228) 688-3832
ramona.e.travis@ssc.nasa.gov

NASA Headquarters

Daniel Lockney,
Technology Transfer Program Executive
(202) 358-2037
daniel.p.lockney@nasa.gov

Small Business Innovation Research (SBIR) & Small Business Technology Transfer (STTR) Programs

Rich Leshner, Program Executive
(202) 358-4920
rleshner@nasa.gov



TECH BRIEFS

NATIONAL AERONAUTICS AND SPACE ADMINISTRATION



5 Technology Focus: Sensors

- 5 Dielectrophoresis-Based Particle Sensor Using Nanoelectrode Arrays
- 5 Multi-Dimensional Damage Detection for Surfaces and Structures
- 6 ULTRA: Underwater Localization for Transit and Reconnaissance Autonomy
- 6 Autonomous Cryogenic Leak Detector for Improving Launch Site Operations
- 7 Submillimeter Planetary Atmospheric Chemistry Exploration Sounder



9 Manufacturing & Prototyping

- 9 Method for Reduction of Silver Biocide Plating on Metal Surfaces
- 9 Silicon Micromachined Microlens Array for THz Antennas



11 Electronics/Computers

- 11 Forward-Looking IED Detector Ground Penetrating Radar
- 11 Fully Printed, Flexible, Phased Array Antenna for Lunar Surface Communication
- 12 Battery Charge Equalizer with Transformer Array
- 12 An Efficient, Highly Flexible Multi-Channel Digital Downconverter Architecture
- 13 Dimmable Electronic Ballast for a Gas Discharge Lamp



15 Materials & Coatings

- 15 Conductive Carbon Nanotube Inks for Use with Desktop Inkjet Printing Technology
- 15 Enhanced Schapery Theory Software Development for Modeling Failure of Fiber-Reinforced Laminates
- 16 High-Performance, Low-Temperature-Operating, Long-Lifetime Aerospace Lubricants
- 16 Carbon Nanotube Microarrays Grown on Nanoflake Substrates
- 17 Differential Muon Tomography to Continuously Monitor Changes in the Composition of Subsurface Fluids



19 Mechanics/Machinery

- 19 Microgravity Drill and Anchor System
- 20 Granular Media-Based Tunable Passive Vibration Suppressor
- 21 Miga Aero Actuator and 2D Machined Mechanical Binary Latch



23 Physical Sciences

- 23 Micro-XRF for *In Situ* Geological Exploration of Other Planets
- 23 Hydrogen-Enhanced Lunar Oxygen Extraction and Storage Using Only Solar Power
- 24 Uplift of Ionospheric Oxygen Ions During Extreme Magnetic Storms
- 24 Miniaturized, High-Speed, Modulated X-Ray Source
- 25 Hollow-Fiber Spacesuit Water Membrane Evaporator
- 25 High-Power Single-Mode 2.65- μm InGaAsSb/AlInGaAsSb Diode Lasers
- 26 Optical Device for Converting a Laser Beam Into Two Co-aligned but Oppositely Directed Beams
- 26 A Hybrid Fiber/Solid-State Regenerative Amplifier with Tunable Pulse Widths for Satellite Laser Ranging
- 27 X-Ray Diffractive Optics



29 Software

- 29 SynGenics Optimization System (SynOptSys)
- 29 CFD Script for Rapid TPS Damage Assessment
- 29 radEq Add-On Module for CFD Solver Loci-CHEM
- 29 Science Opportunity Analyzer (SOA) Version 8
- 30 Autonomous Byte Stream Randomizer



31 Information Technology

- 31 Distributed Engine Control Empirical/Analytical Verification Tools
- 31 Dynamic Server-Based KML Code Generator Method for Level-of-Detail Traversal of Geospatial Data
- 32 Automated Planning of Science Products Based on Nadir Overflights and Alerts for Onboard and Ground Processing
- 32 Linked Autonomous Interplanetary Satellite Orbit Navigation
- 33 Risk-Constrained Dynamic Programming for Optimal Mars Entry, Descent, and Landing
- 33 Scheduling Operations for Massive Heterogeneous Clusters
- 34 Deepak Condenser Model (DeCoM)
- 34 Flight Software Math Library



35 Books & Reports

- 35 Recirculating 1-K-Pot for Pulse-Tube Cryostats
- 35 Method for Processing Lunar Regolith Using Microwaves
- 35 Wells for *In Situ* Extraction of Volatiles from Regolith (WIEVR)
- 35 Estimating the Backup Reaction Wheel Orientation Using Reaction Wheel Spin Rates Flight Telemetry from a Spacecraft

This document was prepared under the sponsorship of the National Aeronautics and Space Administration. Neither the United States Government nor any person acting on behalf of the United States Government assumes any liability resulting from the use of the information contained in this document, or warrants that such use will be free from privately owned rights.



Dielectrophoresis-Based Particle Sensor Using Nanoelectrode Arrays

An array of nanostructure electrodes can provide a more sensitive reading than conventional microelectrodes.

Ames Research Center, Moffett Field, California

A method has been developed for concentrating, or partly separating, particles of a selected species from a liquid or gas containing these particles, and flowing in a channel. An example of this is to promote an accumulation (and thus concentration) of the selected particle (e.g., biological species such as *E. coli*, salmonella, anthrax, tobacco mosaic virus or herpes simplex, and non-biological materials such as nano- and micro-particles, quantum dots, nanowires, nanotubes, and other inorganic particles) adjacent to the first surface.

Additionally, this method can also determine if the particle species is present in the liquid. This is accomplished by providing an insulating material in an interstitial volume between two or more adjacent nanostructure electrodes. It can also be accomplished by providing a functionalizing substance, located on a selected region of the insulating material surface, which promotes attachment of the selected species particles to the functional-

ized surface, and measuring a selected electrical property such as electrical impedance, conductance, or capacitance.

A time-varying electrical field E , having a root-mean-square intensity of E^2 rms, with a non-zero gradient in a direction transverse to the liquid or fluid flow direction, is produced by a nanostructure electrode array with a very high-magnitude gradient near exposed electrode tips. A dielectrophoretic force causes the selected particles to accumulate near the electrode tips, if the medium and selected particles have substantially different dielectric constants. An insulating material surrounds most of the nanostructure electrodes, and a region of the insulating material surface is functionalized to promote attachment of the selected particle species to the surface. An electrical property value $Z(\text{meas})$ is measured at the functionalized surface, and is compared with a reference value $Z(\text{ref})$ to determine if the selected

species particles are attached to the functionalized surface.

Some advantages of this innovation are that an array of nanostructure electrodes can provide an electric field intensity gradient that is one or more orders of magnitude greater than the corresponding gradient provided by a conventional microelectrode arrangement, and that, as a result of the high-magnitude field intensity gradients, a nanostructure concentrator can trap particles from high-speed microfluidic flows. This is critical for applications where the entire analysis must be performed in a few minutes.

This work was done by Jun Li, Alan M. Cassell, and Prabhu U. Arumugam of Ames Research Center. Further information is contained in a TSP (see page 1). Inquiries concerning rights for the commercial use of this invention should be addressed to the Ames Technology Partnerships Division at 1-855-NASA-BIZ (1-855-6272-249). Refer to ARC-15967-1.

Multi-Dimensional Damage Detection for Surfaces and Structures

This system determines the size, depth, and location of damage in a multi-layered system.

John F. Kennedy Space Center, Florida

Current designs for inflatable or semi-rigidized structures for habitats and space applications use a multiple-layer construction, alternating thin layers with thicker, stronger layers, which produces a layered composite structure that is much better at resisting damage. Even though such composite structures or layered systems are robust, they can still be susceptible to penetration damage.

The ability to detect damage to surfaces of inflatable or semi-rigid habitat structures is of great interest to NASA. Damage caused by impacts of foreign

objects such as micrometeorites can rupture the shell of these structures, causing loss of critical hardware and/or the life of the crew. While not all impacts will have a catastrophic result, it will be very important to identify and locate areas of the exterior shell that have been damaged by impacts so that repairs (or other provisions) can be made to reduce the probability of shell wall rupture. This disclosure describes a system that will provide real-time data regarding the health of the inflatable shell or rigidized structures, and information

related to the location and depth of impact damage.

The innovation described here is a method of determining the size, location, and direction of damage in a multi-layered structure. In the multi-dimensional damage detection system, layers of two-dimensional thin film detection layers are used to form a layered composite, with non-detection layers separating the detection layers. The non-detection layers may be either thicker or thinner than the detection layers. The thin-film damage detection layers are

thin films of materials with a conductive grid or striped pattern. The conductive pattern may be applied by several methods, including printing, plating, sputtering, photolithography, and etching, and can include as many detection layers that are necessary for the structure construction or to afford the detection detail level required. The damage is detected using a detector or sensory system, which may include a time domain reflectometer, resistivity monitoring hardware, or other resistance-based systems.

To begin, a layered composite consisting of thin-film damage detection layers separated by non-damage detection layers is fabricated. The damage detection layers are attached to a detector that provides details regarding the physical health of each detection layer individually. If dam-

age occurs to any of the detection layers, a change in the electrical properties of the detection layers damaged occurs, and a response is generated. Real-time analysis of these responses will provide details regarding the depth, location, and size estimation of the damage. Multiple damages can be detected, and the extent (depth) of the damage can be used to generate prognostic information related to the expected lifetime of the layered composite system.

The detection system can be fabricated very easily using off-the-shelf equipment, and the detection algorithms can be written and updated (as needed) to provide the level of detail needed based on the system being monitored. Connecting to the thin film detection layers is very easy as well. The truly unique feature of the system is its flexibility; the system can be designed to gather as much (or as little) in-

formation as the end user feels necessary. Individual detection layers can be turned on or off as necessary, and algorithms can be used to optimize performance. The system can be used to generate both diagnostic and prognostic information related to the health of layer composite structures, which will be essential if such systems are utilized for space exploration. The technology is also applicable to other in-situ health monitoring systems for structure integrity.

This work was done by Martha Williams, Mark Lewis, and Luke Roberson of Kennedy Space Center; and Pedro Medelius, Tracy Gibson, Steven Parks, and Sarah Snyder of ASRC Aerospace Corporation. For further information, contact the KSC Technology Transfer Office at (321) 867-5033. Refer to KSC-13588.

ULTRA: Underwater Localization for Transit and Reconnaissance Autonomy

NASA's Jet Propulsion Laboratory, Pasadena, California

This software addresses the issue of underwater localization of unmanned vehicles and the inherent drift in their onboard sensors. The software gives a 2 to 3 factor of improvement over the state-of-the-art underwater localization algorithms.

The software determines the localization (position, heading) of an AUV (autonomous underwater vehicle) in environments where there is no GPS signal. It accomplishes this using only the commanded position, onboard gyros/accelerometers, and the bathymetry of the bottom provided by an onboard sonar

system. The software does not rely on an onboard bathymetry dataset, but instead incrementally determines the position of the AUV while mapping the bottom.

In order to enable long-distance underwater navigation by AUVs, a localization method called ULTRA uses registration of the bathymetry data products produced by the onboard forward-looking sonar system for hazard avoidance during a transit to derive the motion and pose of the AUV in order to correct the DR (dead reckoning) estimates. The registration algorithm uses iterative point matching (IPM)

combined with surface interpolation of the Iterative Closest Point (ICP) algorithm. This method was used previously at JPL for onboard unmanned ground vehicle localization, and has been optimized for efficient computational and memory use.

This work was done by Terrance L. Huntsberger of Caltech for NASA's Jet Propulsion Laboratory. Further information is contained in a TSP (see page 1).

This software is available for commercial licensing. Please contact Dan Broderick at Daniel.F.Broderick@jpl.nasa.gov. Refer to NPO-48559.

Autonomous Cryogenic Leak Detector for Improving Launch Site Operations

Virtually all storage tanks of hydrogen and other flammable gases could use this sensor technology.

John F. Kennedy Space Center, Florida

NASA, military, and commercial satellite users need launch services that are highly reliable, less complex, easier to test, and cost effective. This project has developed a tapered optical fiber sensor for detecting hydrogen. The invention

involves incorporating chemical indicators on the tapered end of an optical fiber using organically modified silicate nanomaterials.

The Hazardous Gas Detection Lab (HGDL) at Kennedy Space Center is in-

involved in the design and development of instrumentation that can detect and qualify various mission-critical chemicals. Historically, hydrogen, helium, nitrogen, oxygen, and argon are the first five gases of HGDL focus. The use of

these cryogenic fluids in the area of propulsion offers challenges. Due to their extreme low temperatures, these fluids induce contraction of the materials they contact, a potential cause of leakage. Among them, hydrogen is of particular concern.

Small sensors are needed in multiple locations without adding to the structural weight. The most vulnerable parts of the engine are the connection flanges on the transfer lines, which have to support cycles of large thermal amplitude. The thermal protection of the engine provides a closed area, increasing the likelihood of an ex-

plosive atmosphere. Thus, even a small leak represents an unacceptable hazardous condition during loading operations, in flight, or after an aborted launch.

Tapered fibers were first fabricated from 1/1.3-mm core/cladding (silica/plastic) optical fibers. Typically a 1-ft (≈ 30 -cm) section of the 1-mm fiber is cut from the bundle and marked with a pen into five 2- $\frac{1}{4}$ -in. (≈ 5.7 -cm) sections. A propane torch is applied at every alternate mark to burn the jacket and soften the glass core. While the core is softening, the two ends of the fiber are pulled apart slowly to create fine tapers of $\frac{1}{4}$ - to $\frac{1}{2}$ -in. (≈ 6 - to 12-

mm) long on the 1-mm optical fiber. Following this, the non-tapered ends of the fibers are polished to a 0.3-micron finish. Then these fibers were coated with indicators sensitive to hydrogen.

The tapered hydrogen detection system with its unique flexibility is the only system that can be placed in many locations inside the vehicles and detect the exact location of leaks, saving millions of dollars for launch vehicle industries.

This work was done by Kisholoy Goswami of Innosense LLC for Kennedy Space Center. Further information is contained in a TSP (see page 1). KSC-13436

Submillimeter Planetary Atmospheric Chemistry Exploration Sounder

NASA's Jet Propulsion Laboratory, Pasadena, California

A report describes the Submillimeter Planetary Atmospheric Chemistry Exploration Sounder (SPACES), a high-sensitivity laboratory breadboard for a spectrometer targeted at orbital planetary atmospheric analysis. The frequency range is 520 to 590 GHz, with a target noise temperature sensitivity of 2,500 K for detecting water, sulfur compounds, carbon compounds, and other atmospheric constituents. SPACES is a prototype for a powerful tool for the exploration of the chemistry and dynamics of any planetary atmosphere. It is fundamentally a single-pixel receiver

for spectral signals emitted by the relevant constituents, intended to be fed by a fixed or movable telescope/antenna. Its front-end sensor translates the received signal down to the 100-MHz range where it can be digitized and the data transferred to a spectrum analyzer for processing, spectrum generation, and accumulation.

The individual microwave and submillimeter wave components (mixers, LO high-powered amplifiers, and multipliers) of SPACES were developed in cooperation with other programs, although with this type of instrument in mind.

Compared to previous planetary and Earth science instruments, its broad bandwidth ($\approx 13\%$) and rapid tunability (≈ 10 ms) are new developments only made possible recently by the advancement in submillimeter circuit design and processing at JPL.

This work was done by Erich T. Schlecht, Mark A. Allen, John J. Gill, Choonsup Lee, Robert H. Lin, Seth Sin, Imran Mehdi, and Peter H. Siegel of Caltech; and Alain Maestrini of the Observatoire de Paris for NASA's Jet Propulsion Laboratory. Further information is contained in a TSP (see page 1). NPO-48207



Method for Reduction of Silver Biocide Plating on Metal Surfaces

Lyndon B. Johnson Space Center, Houston, Texas

Silver ions in aqueous solutions (0.05 to 1 ppm) are used for microbial control in water systems. The silver ions remain in solution when stored in plastic containers, but the concentration rapidly decreases to non-biocidal levels when stored in metal containers. The silver deposits onto the surface and is reduced to non-biocidal silver metal when it contacts less noble metal surfaces, including stainless steel, titanium, and nickel-based alloys.

Five methods of treatment of contact metal surfaces to deter silver deposition and reduction are proposed:

1. High-temperature oxidation of the metal surface;
2. High-concentration silver solution pre-treatment;
3. Silver plating;
4. Teflon coat by vapor deposition (titanium only); and
5. A combination of methods (1) and (2), which proved to be the best method for the nickel-based alloy application.

The mechanism associated with surface treatments (1), (2), and (5) is thought to be the development of a less active oxide layer that deters ionic silver deposition. Mechanism (3) is an attempt to develop an equilibrium ionic silver concentration via dissolution of metallic silver. Mechanism (4) provides a non-reactive barrier to deter ionic silver plating.

Development testing has shown that ionic silver in aqueous solution was maintained at essentially the same level of addition (0.4 ppm) for up to 15 months with method (5) (a combination of methods (1) and (2)), before the test was discontinued for nickel-based alloys. Method (1) resulted in the maintenance of a biocidal level (approximately 0.05 ppm) for up to 10 months before that test was discontinued for nickel-based alloys. Methods (1) and (2) used separately were able to maintain ionic silver in aqueous solution at essentially the same level of addition (0.4 ppm) for up to 10 months before the test was discontinued for stainless steel alloys. Method (3) was only utilized for titanium

alloys, and was successful at maintaining ionic silver in aqueous solution at essentially the same level of addition (0.4 ppm) for up to 10 months before the test was discontinued for simple flat geometries, but not for geometries that are difficult to Teflon coat.

This work was done by John Steele, Timothy Nalette, and Durwood Beringer of Hamilton Sundstrand for Lockheed Martin under contract with Johnson Space Center. For further information, contact the JSC Innovation Partnerships Office at (281) 483-3809.

Title to this invention has been waived under the provisions of the National Aeronautics and Space Act (42 U.S.C. 2457(f)) to Hamilton Sundstrand. Inquiries concerning licenses for its commercial development should be addressed to:

*Hamilton Sundstrand
One Hamilton Road
Windsor Locks, CT 06096-1010
Phone No.: (860) 654-6000*

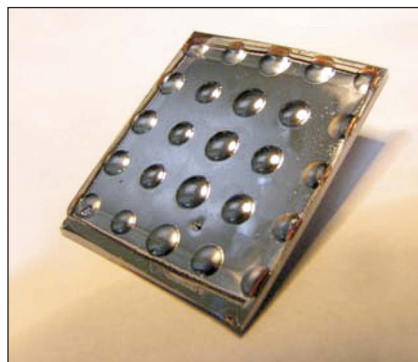
Refer to MSC-24875-1, volume and number of this NASA Tech Briefs issue, and the page number.

Silicon Micromachined Microlens Array for THz Antennas

There is strong demand for a multi-pixel heterodyne detector array for Earth observation, astrophysics, future planetary, and ground applications.

NASA's Jet Propulsion Laboratory, Pasadena, California

A 5x5 silicon microlens array was developed using a silicon micromachining technique for a silicon-based THz antenna array. The feature of the silicon micromachining technique enables one to microfabricate an unlimited number of microlens arrays at one time with good uniformity on a silicon wafer. This technique will resolve one of the key issues in building a THz camera, which is to integrate antennas in a detector array. The conventional approach of building single-pixel receivers and stacking them to form a multi-pixel receiver is not suited at THz because a single-pixel receiver already has difficulty fitting into mass, volume, and power budgets, especially in space applications.



Photograph of Silicon Microlens Array Antenna. The reason why there are different sizes of silicon microlenses is that each column has a different diameter of microlens on the mask plate. The microlens diameter of each column is very uniform.

In this proposed technique, one has controllability on both diameter and curvature of a silicon microlens. First of all, the diameter of microlens depends on how thick photoresist one could coat and pattern. So far, the diameter of a 6-mm photoresist microlens with 400 μm in height has been successfully microfabricated. Based on current researchers' experiences, a diameter larger than 1-cm photoresist microlens array would be feasible.

In order to control the curvature of the microlens, the following process variables could be used:

1. Amount of photoresist: It determines the curvature of the photoresist microlens. Since the photoresist lens is

transferred onto the silicon substrate, it will directly control the curvature of the silicon microlens.

2. Etching selectivity between photoresist and silicon: The photoresist microlens is formed by thermal reflow. In order to transfer the exact photoresist curvature onto silicon, there needs to be etching selectivity of 1:1 between silicon and photoresist. However, by varying the etching selectivity, one could control the curvature of the silicon microlens.

The figure shows the microfabricated silicon microlens 5×5 array. The diameter of the microlens located in the center is about 2.5 mm. The measured 3-D profile of the microlens surface has a

smooth curvature. The measured height of the silicon microlens is about 280 μm. In this case, the original height of the photoresist was 210 μm. The change was due to the etching selectivity of 1.33 between photoresist and silicon. The measured surface roughness of the silicon microlens shows the peak-to-peak surface roughness of less than 0.5 μm, which is adequate in THz frequency. For example, the surface roughness should be less than 7 μm at 600 GHz range. The SEM (scanning electron microscope) image of the microlens confirms the smooth surface. The beam pattern at 550 GHz shows good directivity.

This work was done by Choonsup Lee, Goutam Chattopadhyay, Imran Mehdi, John

J. Gill, and Cecile D. Jung-Kubiak of Caltech; and Nuria Llombart of the Universidad Complutense de Madrid, Spain, for NASA's Jet Propulsion Laboratory. Further information is contained in a TSP (see page 1).

In accordance with Public Law 96-517, the contractor has elected to retain title to this invention. Inquiries concerning rights for its commercial use should be addressed to:

*Innovative Technology Assets Management
JPL*

*Mail Stop 321-123
4800 Oak Grove Drive
Pasadena, CA 91109-8099*

E-mail: iaoffice@jpl.nasa.gov

Refer to NPO-48017, volume and number of this NASA Tech Briefs issue, and the page number.



Forward-Looking IED Detector Ground Penetrating Radar

This convoy-mounted IED detector radar could be used on route-clearing vehicles.

NASA's Jet Propulsion Laboratory, Pasadena, California

There have been many developments of mine or metal detectors based on ground penetrating radar techniques, usually in handheld or rover-mounted devices. In most mine or metal detector applications, conditions are in a stationary mode and detection speed is not an important factor.

A novel, forward-looking, stepped-frequency ground penetrating radar (GPR) has been developed with a capability to detect improvised explosive devices (IEDs) at vehicular speeds of 15 to 20 mi/h (24 to 32 km/h), 10 to 20 m ahead of the vehicle, to ensure adequate time for response. The GPR system employs two horn antennas (1.7 to 2.6 GHz, 20 dBi) as transmit and receive. The detector system features a user-friendly instantaneous display on a laptop PC and is a low-power-consumption (3 W) compact system with minimal impact on vehicle operations. In practice, the whole GPR system and a laptop PC can be powered by plugging into a cigarette lighter of a vehicle.

The stepped-frequency continuous-wave (CW) radar scans frequency from 1.7 to 2.6 GHz in 1,000 steps of 0.9 MHz, with the full frequency scan in 60 ms. The GPR uses a bi-static configuration with one horn antenna used as a transmitter and the other used as a receiver so that isolation between transmitter and receiver is improved. Since the horn antennas (20 dBi) are mounted on the roof of a vehicle at a shallow inclination angle (15 to 25° with respect to horizontal), there is a first-order reduction in ground reflection so that a significant amount of the total reflected power received by the GPR comes from the scattering of RF energy off of buried objects.

The stepped-frequency technique works by transmitting a tone at a particular frequency, while the received signal is mixed with the transmitted tone. As a result, the output of the mixer produces a signal that indicates the strength of the received signal and the extent to which it is in phase or out of phase with the

transmitted tone. By taking measurements of the phase relationship between the transmitted and received signals over a wide frequency range, an interference pattern is produced showing all target reflections. When a Fourier transform is performed on this pattern, the result is a time-domain representation of targets. Among the advantages of this technique over impulse radar is the ability to transmit and receive much more total energy, and to use non-damped, highly focused horn antennas.

The novelty of the IED detector GPR has been achieved by miniaturization of GPR electronics (single electronics board, 10×5×2 cm), low power consumption (3 W), faster signal processing capability, and minimal impact on vehicle operations.

This work was done by Soon Sam Kim and Steven R. Carnes of Caltech, and Christopher T. Ulmer of Ulmer Systems, Inc. for NASA's Jet Propulsion Laboratory. For more information, contact iaoffice@jpl.nasa.gov. Refer to NPO-47028.

Fully Printed, Flexible, Phased Array Antenna for Lunar Surface Communication

Applications include RFID tags, sensors, smart cards, electronic paper, and large-area flat-panel displays.

John H. Glenn Research Center, Cleveland, Ohio

NASA's future exploration missions focus on the manned exploration of the Moon, Mars, and beyond, which will rely heavily on the development of a reliable communications infrastructure from planetary surface-to-surface, surface-to-orbit, and back to Earth. Flexible antennas are highly desired in many scenarios.

Active phased array antennas (active PAAs) with distributed control and processing electronics at the surface of an antenna aperture offer numerous advantages for radar communications. Large-area active PAAs on flexible substrates are of particular interest in

NASA's space radars due to their efficient inflatable package that can be rolled up during transportation and deployed in space. Such an inflatable package significantly reduces stowage volume and mass. Because of these performance and packaging advantages, large-area inflatable active PAAs are highly desired in NASA's surface-to-orbit and surface-to-relay communications.

To address the issues of flexible electronics, a room-temperature printing process of active phased-array antennas on a flexible Kapton substrate was developed. Field effect transistors (FETs) based

on carbon nanotubes (CNTs), with many unique physical properties, were successfully proved feasible for the PAA system.

This innovation is a new type of fully inkjet-printable, two-dimensional, high-frequency PAA on a flexible substrate at room temperature. The designed electronic circuit components, such as the FET switches in the phase shifter, metal interconnection lines, microstrip transmission lines, etc., are all printed using a special inkjet printer. Using the developed technology, entire 1×4, 2×2, and 4×4 PAA systems were developed, packaged, and demonstrated at 5.3 GHz.

Several key solutions are addressed in this work to solve the fabrication issues. The source/drain contact is developed using droplets of silver ink printed on the source/drain areas prior to applying CNT thin-film. The wet silver ink droplets allow the silver to “wet” the CNT thin-film area and enable good contact with the source and drain contact after annealing. A passivation layer to protect the device channel is developed by bonding a thin Kapton film on top of the device channel. This film is also used as the media for transferring the aligned CNT thin-film on the device substrate.

A simple and cost-effective technique to form multilayer metal interconnections on flexible substrate is developed and demonstrated. Contact vias are formed on the second substrate prior to bonding on the first substrate. Inkjet printing is used to fill the silver ink into the via structure. The printed silver ink penetrates through the vias to contact with the contact pads on the bottom layer. It is then annealed to form a good connection. One-dimensional and two-dimensional PAAs were fabricated and characterized. In these circuits, multilayer metal

interconnects were used to make a complete PAA system.

This work was done by Harish Subbaraman of Omega Optics, Inc., Ray T. Chen of the University of Texas at Austin, Xuejun Lu of University of Massachusetts – Lowell, and Maggie Yihong Chen of Texas State University for Glenn Research Center. Further information is contained in a TSP (see page 1).

Inquiries concerning rights for the commercial use of this invention should be addressed to NASA Glenn Research Center, Innovative Partnerships Office, Attn: Steven Fedor, Mail Stop 4–8, 21000 Brookpark Road, Cleveland, Ohio 44135. Refer to LEW-19035-1.

Battery Charge Equalizer with Transformer Array

Lyndon B. Johnson Space Center, Houston, Texas

High-power batteries generally consist of a series connection of many cells or cell banks. In order to maintain high performance over battery life, it is desirable to keep the state of charge of all the cell banks equal. A method provides individual charging for battery cells in a large, high-voltage battery array with a minimum number of transformers while maintaining reasonable efficiency. This is designed to augment a simple high-current charger that supplies the main charge energy.

The innovation will form part of a larger battery charge system. It consists of a transformer array connected to the

battery array through rectification and filtering circuits. The transformer array is connected to a drive circuit and a timing and control circuit that allow individual battery cells or cell banks to be charged. The timing circuit and control circuit connect to a charge controller that uses battery instrumentation to determine which battery bank to charge. It is important to note that the innovation can charge an individual cell bank at the same time that the main battery charger is charging the high-voltage battery.

The fact that the battery cell banks are at a non-zero voltage, and that they are

all at similar voltages, can be used to allow charging of individual cell banks. A set of transformers can be connected with secondary windings in series to make weighted sums of the voltages on the primaries.

This work was done by Francis Davies of Johnson Space Center. Further information is contained in a TSP (see page 1).

This invention is owned by NASA, and a patent application has been filed. Inquiries concerning nonexclusive or exclusive license for its commercial development should be addressed to the Patent Counsel, Johnson Space Center, (281) 483-1003. Refer to MSC-25026-1.

An Efficient, Highly Flexible Multi-Channel Digital Downconverter Architecture

This technology can be used for any digital recording device that requires a flexible way to break a large input bandwidth into many smaller channels.

NASA's Jet Propulsion Laboratory, Pasadena, California

In this innovation, a digital downconverter has been created that produces a large (16 or greater) number of output channels of smaller bandwidths. Additionally, this design has the flexibility to tune each channel independently to anywhere in the input bandwidth to cover a wide range of output bandwidths (from 32 MHz down to 1 kHz). Both the flexibility in channel frequency selection and the more than four orders of magnitude range in output bandwidths (decimation rates from

32 to 640,000) presented significant challenges to be solved.

The solution involved breaking the digital downconversion process into a two-stage process. The first stage is a 2× oversampled filter bank that divides the whole input bandwidth as a real input signal into seven overlapping, contiguous channels represented with complex samples. Using the symmetry of the sine and cosine functions in a similar way to that of an FFT (fast Fourier transform), this downconver-

sion is very efficient and gives seven channels fixed in frequency. An arbitrary number of smaller bandwidth channels can be formed from second-stage downconverters placed after the first stage of downconversion.

Because of the overlapping of the first stage, there is no gap in coverage of the entire input bandwidth. The input to any of the second-stage downconverting channels has a multiplexer that chooses one of the seven wideband channels from the first stage. These second-stage

downconverters take up fewer resources because they operate at lower bandwidths than doing the entire downconversion process from the input bandwidth for each independent channel. These second-stage downconverters are each independent with fine frequency control tuning, providing extreme flexibility in positioning the center frequency of a downconverted channel. Finally, these second-stage downconverters have flexible decimation factors over four orders of magnitude.

The algorithm was developed to run in an FPGA (field programmable gate array) at input data sampling rates of up to 1,280 MHz. The current implementation takes a 1,280-MHz real input, and first breaks it up into seven 160-MHz complex channels, each spaced 80 MHz apart. The eighth channel at baseband was not required for this implementation, and led to more optimization. Afterwards, 16 second stage narrow band channels with independently tunable center frequencies and bandwidth settings are implemented.

A future implementation in a larger Xilinx FPGA will hold up to 32 independent second-stage channels.

This work was done by Charles E. Goodhart, Melissa A. Soriano, Robert Navarro, Joseph T. Trinh, and Elliott H. Sigman of Caltech for NASA's Jet Propulsion Laboratory. Further information is contained in a TSP (see page 1).

The software used in this innovation is available for commercial licensing. Please contact Dan Broderick at Daniel.F.Broderick@jpl.nasa.gov. Refer to NPO-47431.

Dimmable Electronic Ballast for a Gas Discharge Lamp

Lyndon B. Johnson Space Center, Houston, Texas

Titanium dioxide (TiO₂) is the most efficient photocatalyst for organic oxidative degradation. TiO₂ is effective not only in aqueous solution, but also in non-aqueous solvents and in the gas phase. It is photostable, biologically and chemically inert, and non-toxic. Low-energy UV light (approximately 375 nm, UV-A) can be used to photoactivate TiO₂. TiO₂ photocatalysis has been used to mineralize most types of organic compounds. Also, TiO₂ photocatalysis has been effectively used in sterilization. This effectiveness has been demonstrated by its aggressive destruction of microorganisms, and aggressive oxidation effects of toxins. It also has been used for the oxidation of carbon monoxide to carbon dioxide, and ammonia to nitrogen.

Despite having many attractive features, advanced photocatalytic oxidation processes have not been effectively used for air cleaning. One of the limitations of the traditional photocatalytic systems is the ballast that powers (lights) the bulbs. Almost all commercial off-the-shelf (COTS) ballasts are not dimmable and do not contain safety features. COTS ballasts light the UV lamp as bright as the bulb can be lit, and this results in shorter bulb lifetime and maximal power consumption. COTS magnetic ballasts are bulky, heavy, and inefficient.

Several iterations of dimmable electronic ballasts have been developed. Some manifestations have safety features such as broken-bulb or over-tempera-

ture warnings, replace-bulb alert, log-bulb operational hours, etc.

Several electronic ballast boards capable of independently lighting and controlling (dimming) four fluorescent (UV light) bulbs were designed, fabricated, and tested. Because of the variation in the market bulb parameters, the ballast boards were designed with a very broad range output. The ballast boards can measure and control the current (power) for each channel.

This work was done by Marius Raducanu and Brian D. Hennings of Lynntech, Inc. for Johnson Space Center. For further information, contact the JSC Innovation Partnerships Office at (281) 483-3809. MSC-24333-1



Conductive Carbon Nanotube Inks for Use with Desktop Inkjet Printing Technology

A mixture of carbon nanotubes and silver or gold nanoparticles could be applied by inkjet printing to flexible substrates.

John F. Kennedy Space Center, Florida

Inkjet printing is a common commercial process. In addition to the familiar use in printing documents from computers, it is also used in some industrial applications. For example, wire manufacturers are required by law to print the wire type, gauge, and safety information on the exterior of each foot of manufactured wire, and this is typically done with inkjet or laser printers.

The goal of this work was the creation of conductive inks that can be applied to a wire or flexible substrates via inkjet printing methods. The use of inkjet printing technology to print conductive inks has been in testing for several years. While researchers have been able to get the printing system to mechanically work, the application of conductive inks on substrates has not consistently produced adequate low resistances in the kilohm range.

Conductive materials can be applied using a printer in single or multiple passes onto a substrate including textiles, polymer films, and paper. The conduc-

tive materials are composed of electrical conductors such as carbon nanotubes (including functionalized carbon nanotubes and metal-coated carbon nanotubes); graphene, a polycyclic aromatic hydrocarbon (e.g., pentacene and bis-peripentacene); metal nanoparticles; inherently conductive polymers (ICP); and combinations thereof. Once the conductive materials are applied, the materials are dried and sintered to form adherent conductive materials on the substrate. For certain formulations, increased conductivity can be achieved by printing on substrates supported by low levels of magnetic field alignment. The adherent conductive materials can be used in applications such as damage detection, dust particle removal, smart coating systems, and flexible electronic circuitry.

By applying alternating layers of different electrical conductors to form a layered composite material, a single homogeneous layer can be produced with improved electrical properties. It is be-

lieved that patterning alternate layers of different conductors may improve electrical pathways through alignment of the conductors and band gap optimization.

One feature of this innovation is that flexible conductive traces could be accomplished with a conductive ink having a surface resistivity of less than 10 ohms/square. Another result was that a composite material comprising a mixture of carbon nanotubes and metallic nanoparticles could be applied by inkjet printing to flexible substrates, and the resulting applied material was one to two orders of magnitude more conductive than a material made by printing inks containing carbon nanotubes alone.

This work was done by Luke Roberson, Martha Williams, LaNetra Tate, Craig Fortier, David Smith, and Kyle Davia of Kennedy Space Center; Tracy Gibson of ASRC Aerospace; and Sarah Snyder of Sierra Lobo. For more information, contact the KSC Technology Transfer Office at (321) 867-5033. KSC-13343

Enhanced Schapery Theory Software Development for Modeling Failure of Fiber-Reinforced Laminates

This tool captures the physics of the damage and failure mechanisms.

John H. Glenn Research Center, Cleveland, Ohio

Progressive damage and failure analysis (PDFA) tools are needed to predict the nonlinear response of advanced fiber-reinforced composite structures. Predictive tools should incorporate the underlying physics of the damage and failure mechanisms observed in the composite, and should utilize as few input parameters as possible.

The purpose of the Enhanced Schapery Theory (EST) was to create a PDFA tool that operates in conjunction with a commercially available finite element (FE) code (Abaqus). The tool cap-

tures the physics of the damage and failure mechanisms that result in the nonlinear behavior of the material, and the failure methodology employed yields numerical results that are relatively insensitive to changes in the FE mesh. The EST code is written in Fortran and compiled into a static library that is linked to Abaqus. A Fortran Abaqus UMAT material subroutine is used to facilitate the communication between Abaqus and EST.

A clear distinction between damage and failure is imposed. Damage mech-

anisms result in pre-peak nonlinearity in the stress strain curve. Four internal state variables (ISVs) are utilized to control the damage and failure degradation. All damage is said to result from matrix microdamage, and a single ISV marks the microdamage evolution as it is used to degrade the transverse and shear moduli of the lamina using a set of experimentally obtainable matrix microdamage functions. Three separate failure ISVs are used to incorporate failure due to fiber breakage, mode I matrix cracking, and mode

II matrix cracking. Failure initiation is determined using a failure criterion, and the evolution of these ISVs is controlled by a set of traction-separation laws. The traction separation laws are postulated such that the area under the curves is equal to the fracture toughness of the material associated with the corresponding failure mechanism. A characteristic finite element length is used to transform the traction-separation laws into stress-strain laws. The ISV

evolution equations are derived in a thermodynamically consistent manner by invoking the stationary principle on the total work of the system with respect to each ISV.

A novel feature is the inclusion of both pre-peak damage and appropriately scaled, post-peak strain softening failure. Also, the characteristic elements used in the failure degradation scheme are calculated using the element nodal coordinates, rather than

simply the square root of the area of the element.

This work was done by Evan J. Pineda of Glenn Research Center and Anthony M. Waas of the University of Michigan. Further information is contained in a TSP (see page 1).

Inquiries concerning rights for the commercial use of this invention should be addressed to NASA Glenn Research Center, Innovative Partnerships Office, Attn: Steven Fedor, Mail Stop 4-8, 21000 Brookpark Road, Cleveland, Ohio 44135. Refer to LEW-18954-1

High-Performance, Low-Temperature-Operating, Long-Lifetime Aerospace Lubricants

John H. Glenn Research Center, Cleveland, Ohio

The synthesis and characterization of six new ionic liquids, with fluoroether moieties on the imidazolium ring, each with vapor pressures shown to be $<10^{-7}$ Torr at 25 °C, have been demonstrated. Thermal stability of the ionic liquids up to 250 °C was demonstrated. The ionic liquids had no measurable influence upon viscosity upon addition to perfluoropolyether (PFPE) base fluids. They also had no measureable influence upon corrosion on steel substrates upon addition to base fluids. In general, 13 to 34% lower COFs (coefficients of friction), and 30 to 80% higher OK load of base

fluids upon addition of the ionic liquids was shown.

The compound consists of a 1,3-disubstituted imidazolium cation. The substituents comprise perfluoroether groups. A bis(trifluoromethanesulfonyl)imide anion counterbalances the charge. The fluorinated groups are intended to enhance dispersion of the ionic liquid in the PFPE base fluid. The presence of weak Van der Waals forces associated with fluorine atoms will limit interaction of the substituents on adjacent ions. The longer interionic distances will reduce the heat of melting

and viscosity, and will increase dispersion capabilities.

This work was done by Bryan Bergeron, David Skyler, Kyle Roberts, and Amy Stevens of Physical Sciences, Inc. for Glenn Research Center. Further information is contained in a TSP (see page 1).

Inquiries concerning rights for the commercial use of this invention should be addressed to NASA Glenn Research Center, Innovative Partnerships Office, Attn: Steven Fedor, Mail Stop 4-8, 21000 Brookpark Road, Cleveland, Ohio 44135. Refer to LEW-19039-1.

Carbon Nanotube Microarrays Grown on Nanoflake Substrates

This process creates materials comprised predominantly of single-walled carbon nanotubes.

Lyndon B. Johnson Space Center, Houston, Texas

This innovation consists of a new composition of matter where single-walled carbon nanotubes (SWNTs) are grown in aligned arrays from nanostructured flakes that are coated in Fe catalyst. This method of growth of aligned SWNTs, which can yield well over 400 percent SWNT mass per unit substrate mass, exceeds current yields for entangled SWNT growth. In addition, processing can be performed with minimal wet etching treatments, leaving aligned SWNTs with superior properties over those that exist in entangled mats.

The alignment of the nanotubes is similar to that achieved in vertically aligned nanotubes, which are called “carpets.” Because these flakes are

grown in a state where they are airborne in a reactor, these flakes, after growing SWNTs, are termed “flying carpets.”

These flakes are created in a roll-to-roll evaporator system, where three subsequent evaporations are performed on a 100-ft (≈ 30 -m) roll of Mylar. The first layer is composed of a water-soluble “release layer,” which can be a material such as NaCl. After depositing NaCl, the second layer involves 40 nm of supporting layer material — either Al_2O_3 or MgO. The thickness of the layer can be tuned to synthesize flakes that are larger or smaller than those obtained with a 40-nm deposition.

Finally, the third layer consists of a thin Fe catalyst layer with a thickness of

0.5 nm. The thickness of this layer ultimately determines the diameter of SWNT growth, and a layer that is too thick will result in the growth of multi-walled carbon nanotubes instead of single-wall nanotubes. However, between a thickness of 0.5 nm to 1 nm, single-walled carbon nanotubes are known to be the primary constituent. After this three-layer deposition process, the Mylar is rolled through a bath of water, which allows catalyst-coated flakes to detach from the Mylar. The flakes are then collected and dried. The method described here for making such flakes is analogous to that which is used to make birefringent ink that is coated on U.S. currency.

After deposition, the growth is carried out in a hot-filament chemical vapor deposition apparatus. A tungsten hot filament placed in the flow of H_2 at a temperature greater than $1,600\text{ }^\circ\text{C}$ creates atomic hydrogen, which serves to reduce the Fe catalyst into a metallic state. The catalyst can now precipitate SWNTs in the presence of growth gases. The gasses used for the experiments reported are C_2H_2 , H_2O , and H_2 , at rates of 2, 2, and 400 standard cubic centimeters per minute (sccm), respectively.

In order to retain the flakes, a cage is constructed by spot welding stainless steel or copper mesh to form an enclosed area, in which the flakes are placed prior to growth. This allows growth gases and atomic hydrogen to reach the flakes, but does not allow the flakes, which rapidly nucleate SWNTs, to escape from the cage.

This work was done by Howard K. Schmidt, Robert H. Hauge, Cary Pint, and Sean Pheasant of Rice University for Johnson Space Center. For further information, contact the JSC Innovation Partnerships Office at

(281) 483-3809.

In accordance with Public Law 96-517, the contractor has elected to retain title to this invention. Inquiries concerning rights for its commercial use should be addressed to:

*Rice University
Office of Technology Transfer MS 705
P.O. Box 1892
Houston, TX 77251-1892
Phone No.: (713) 348-6188
E-Mail: techtran@rice.edu*

Refer to MSC-24500-1, volume and number of this NASA Tech Briefs issue, and the page number.

❏ Differential Muon Tomography to Continuously Monitor Changes in the Composition of Subsurface Fluids

This innovation enables tracking of carbon storage or enhanced oil recovery in subsurface reservoir projects.

NASA's Jet Propulsion Laboratory, Pasadena, California

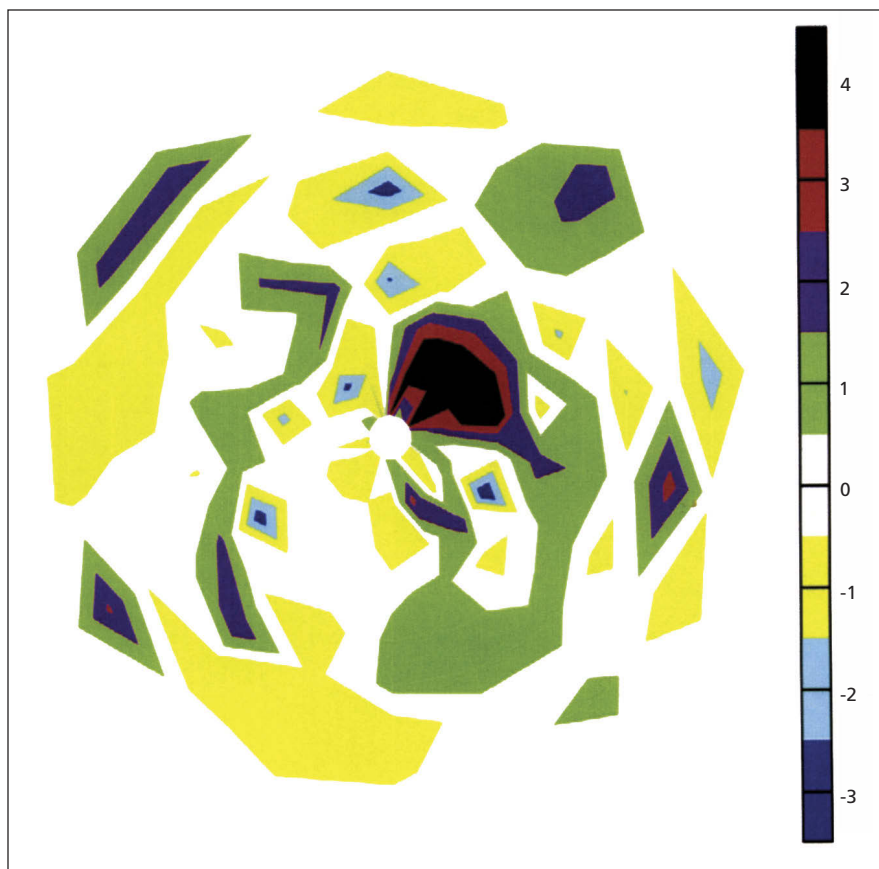
Muon tomography has been used to seek hidden chambers in Egyptian pyramids and image subsurface features in volcanoes. It seemed likely that it could be used to image injected, supercritical carbon dioxide as it is emplaced in porous geological structures being used for carbon sequestration, and also to check on subsequent leakage. It should work equally well in any other application where there are two fluids of different densities, such as water and oil, or carbon dioxide and heavy oil in oil reservoirs.

Continuous monitoring of movement of oil and/or flood fluid during enhanced oil recovery activities for managing injection is important for economic reasons. Checking on leakage for geological carbon storage is essential both for safety and for economic purposes. Current technology (for example, repeat 3D seismic surveys) is expensive and episodic. Muons are generated by high-energy cosmic rays resulting from supernova explosions, and interact with gas molecules in the atmosphere. This innovation has produced a theoretical model of muon attenuation in the thickness of rock above and within a typical sandstone reservoir at a depth of between 1.00 and 1.25 km. Because this first simulation was focused on carbon sequestration, the innovators chose depths sufficient for the pressure there to ensure that the carbon dioxide would be supercritical.

This innovation demonstrates for the first time the feasibility of using the natu-

ral cosmic-ray muon flux to generate continuous tomographic images of carbon dioxide in a storage site. The muon flux is attenuated to an extent dependent on, amongst other things, the density

of the materials through which it passes. The density of supercritical carbon dioxide is only three quarters that of the brine in the reservoir that it displaces. The first realistic simulations indicate



A contour plot of the **Muon Intensity Change** due to CO_2 injection into the reservoir over a period of one year, expressed as standard deviations from the initial value.

that changes as small as 0.4% in the storage site bulk density could be detected (equivalent to 7% of the porosity, in this specific case). The initial muon flux is effectively constant at the surface of the Earth. Sensitivity of the method would be

decreased with increasing depth. However, sensitivity can be improved by emplacing a greater array of particle detectors at the base of the reservoir.

This work was done by Max Coleman of Caltech; Vitaly A. Kudryavtsev, Neil J.

Spooner, and Cora Fung of University of Sheffield; and Jon Ghuyas of University of Durham for NASA's Jet Propulsion Laboratory. Further information is contained in a TSP (see page 1). NPO-48328



Microgravity Drill and Anchor System

This system has applications in rock-climbing and cave exploration, as well as in drilling into rock on the sea floor.

NASA's Jet Propulsion Laboratory, Pasadena, California

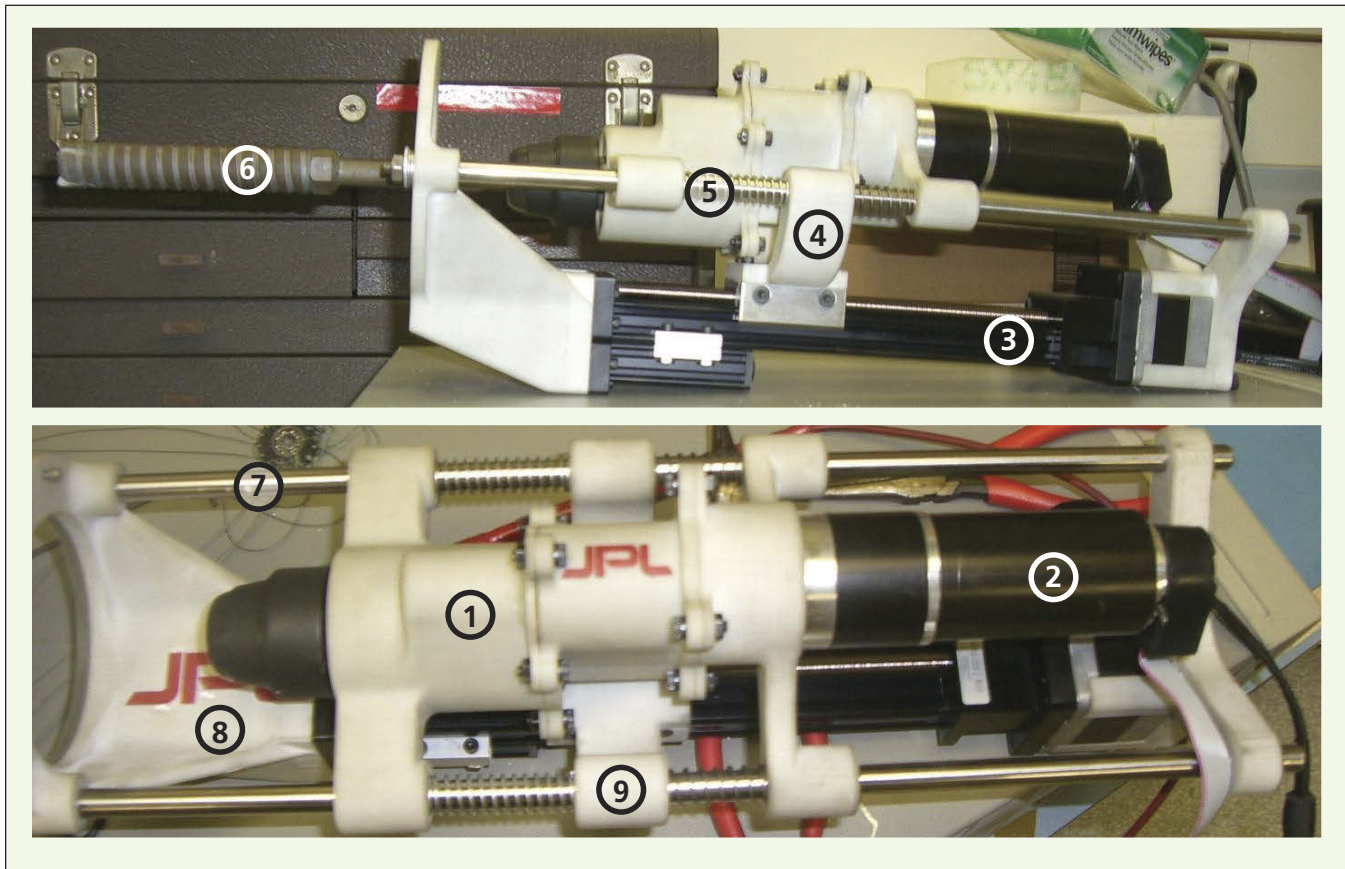
This work is a method to drill into a rock surface regardless of the gravitational field or orientation. The required weight-on-bit (WOB) is supplied by a self-contained anchoring mechanism. The system includes a rotary percussive coring drill, forming a complete sampling instrument usable by robot or human. This method of *in situ* sample acquisition using microspine anchoring technology enables several NASA mission concepts not currently possible with existing technology, including sampling from consolidated rock on asteroids, providing a bolt network for astronauts visiting a near-Earth asteroid, and sampling from the ceilings or vertical walls of lava tubes and cliff faces on Mars.

One of the most fundamental parameters of drilling is the WOB; essentially, the load applied to the bit that allows it to cut, creating a reaction force normal to the surface. In every drilling application, there is a minimum WOB that must be maintained for the system to function properly. In microgravity (asteroids and comets), even a small WOB could not be supported conventionally by the weight of the robot or astronaut. An anchoring mechanism would be needed to resist the reactions, or the robot or astronaut would push themselves off the surface and into space.

The ability of the system to anchor itself to a surface creates potential applications that reach beyond use in low gravity. The use of these anchoring

mechanisms as end effectors on climbing robots has the potential of vastly expanding the scope of what is considered accessible terrain. Further, because the drill is supported by its own anchor rather than by a robotic arm, the workspace is not constrained by the reach of such an arm. Yet, if the drill is on a robotic arm, it has the benefit of not reflecting the forces of drilling back to the arm's joints. Combining the drill with the anchoring feet will create a highly mobile, highly stable, and highly reliable system.

The drilling system's anchor uses hundreds of microspine toes that independently find holes and ledges on a rock to create an anchor. Once the system is anchored, a linear translation mechanism



The top and side views of the assembled **Microgravity Drill** showing (1) the housing, (2) drive motor, (3) linear translation mechanism, (4) slide carriage, (5) compression springs $\times 4$, (6) bit, (7) guide rails $\times 2$, (8) mounting plate, and (9) housed linear bearings $\times 6$.

moves the drill axially into the surface while maintaining the proper WOB. The linear translation mechanism is composed of a ball screw and stepper motor that can translate a carriage with high precision and applied load. The carriage slides along rails using self-aligning linear bearings that correct any axial misalignment caused by bending and torsion. The carriage then compresses a series of springs that simultaneously transmit the load to the drill along the bit axis and act as a suspension that compensates for the vibration caused by percussive drilling.

The drill is a compacted, modified version of an off-the-shelf rotary percussive drill, which uses a custom carbide-tipped

coring bit. By using rotary percussive drilling, the drill time is greatly reduced. The percussive action fractures the rock debris, which is removed during rotation. The final result is a 0.75-in. (≈ 1.9 -cm) diameter hole and a preserved 0.5-in. (≈ 1.3 -cm) diameter rock core.

This work extends microspine technology, making it applicable to astronaut missions to asteroids and a host of robotic sampling concepts. At the time of this reporting, it is the first instrument to be demonstrated using microspine anchors, and is the first self-contained drill/anchor system to be demonstrated that is capable of drilling in inverted configurations and would be capable of drilling in microgravity.

This work was done by Aaron Parness, Matthew A. Frost, and Jonathan P. King of Caltech for NASA's Jet Propulsion Laboratory. Further information is contained in a TSP (see page 1).

In accordance with Public Law 96-517, the contractor has elected to retain title to this invention. Inquiries concerning rights for its commercial use should be addressed to:

*Innovative Technology Assets Management
JPL*

*Mail Stop 202-233
4800 Oak Grove Drive
Pasadena, CA 91109-8099*

*E-mail: iaoffice@jpl.nasa.gov
Refer to NPO-48316, volume and number of this NASA Tech Briefs issue, and the page number.*

Granular Media-Based Tunable Passive Vibration Suppressor

Potential applications include vehicle shock absorbers, earthquake protection systems, and explosion protection systems.

NASA's Jet Propulsion Laboratory, Pasadena, California

A complete, tested, and tunable shock and vibration suppression device is composed of statically compressed chains of spherical particles. The device superimposes a combination of dissipative damping and dispersive effects. The dissipative damping resulting from the elastic wave attenuation properties of the bulk material selected for the granular media is independent of particle geometry and periodicity, and can be accordingly designed based on the dissipative (or viscoelastic) properties of the material. For instance, a viscoelastic polymer might be selected where broadband damping is desired. In contrast, the dispersive effects result from the periodic arrangement and geometry of particles composing a linear granular chain. A uniform (monatomic) chain of statically compressed spherical particles will have a low-pass filter effect, with a cutoff frequency tunable as a function of particle mass, elastic modulus, Poisson's ratio, radius, and static compression. Elastic

waves with frequency content above this cutoff frequency will exhibit an exponential decay in amplitude as a function of propagation distance.

System design targeting a specific application is conducted using a combination of theoretical, computational, and experimental techniques to appropriately select the particle radii, material (and thus elastic modulus and Poisson's ratio), and static compression to satisfy estimated requirements derived for shock and/or vibration protection needs under particular operational conditions. The selection of a chain of polymer spheres with an elastic modulus ≈ 3 provided the appropriate dispersive filtering effect for that exercise; however, different operational scenarios may require the use of other polymers, metals, ceramics, or a combination thereof, configured as an array of spherical particles.

The device is a linear array of spherical particles compressed in a container with a mechanism for attachment to the shock and/or vibration source, and a

mechanism for attachment to the article requiring isolation (Figure 1). This configuration is referred to as a single-axis vibration suppressor. This invention also includes further designs for the integration of the single-axis vibration suppressor into a six-degree-of-freedom hexapod "Stewart" mounting configuration (Figure 2). By integrating each single-axis vibration suppressor into a hexapod formation, a payload will be protected in all six degrees of freedom from shock and/or vibration. Additionally, to further enable the application of this device to multiple operational scenarios, particularly in the case of high loads, the vibration suppressor devices can be used in parallel in any array configuration.

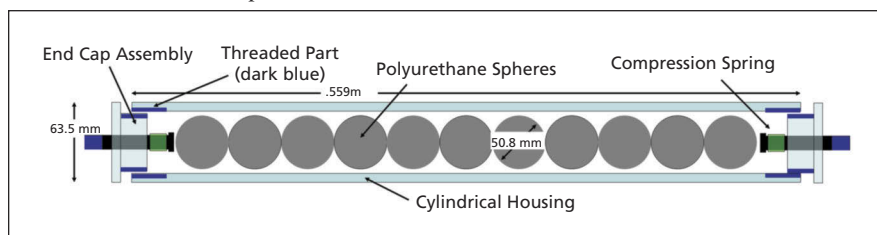


Figure 1. Initial schematic for the **Vibration Suppressor**. Pistons at each end of the cylinder make contact with the granular chain of spheres. Static compression of the granular chain is achieved through the use of soft springs located between the pistons and end caps, which screw onto the container.



Figure 2. **Hexapod Configuration** for spacecraft mounting.

The parallel application of these devices divides the amplitude of the incident vibrations while preserving the frequency content and thus preserving the designed operation of the invention.

This invention includes the design of a novel, self-contained method for adjustably applying (and simply adjusting or tuning) static compression to the chain of spheres while still transmitting vibration through the dissipative and dispersive media. The dispersive filtering effect for this system only exists as predicted in the presence of static compression, which must be applied in application.

However, the mechanical method for applying this compression must be decoupled enough from the vibration source and payload such that vibrations are not primarily transmitted through the static compression mechanism and around the dissipative and dispersive media. This invention utilizes the solution of a soft spring-loaded casing for the chain of spherical particles, designed so

that the first mode of the casing spring mass system is within the pass band of the dispersive filter. Attachment points are coupled directly to the first and last particle of the granular chain for simple attachment in between the payload and vibration source. The soft coupling and low-frequency first mode of the casing ensure the vibrations are transmitted primarily through the filtering media.

Performance of the invention was demonstrated using a prototype single-axis vibration suppressor constructed and tested under both high-amplitude simulated pyroshock and low-amplitude continuous broadband noise perturbations. The results show high attenuation with frequency response characteristics in accordance with the theoretical and numerical predictions. Two orders of magnitude reduction were observed in the shock response spectra at frequencies over 1 kHz, and over two orders of magnitude reduction in the peak accelerations for high-amplitude transient

shocklike impacts. Approximately one order of magnitude reduction in the shock response spectra at frequencies below 1 kHz, which was attributed to the dissipative effects of the bulk polyurethane material, was observed.

This work was done by Robert P. Dillon, Gregory L. Davis, Andrew A. Shapiro, John Paul C. Borgonia, Daniel L. Kahn, Nicholas Boehler, and Chiara Davaio of Caltech for NASA's Jet Propulsion Laboratory. Further information is contained in a TSP (see page 1).

In accordance with Public Law 96-517, the contractor has elected to retain title to this invention. Inquiries concerning rights for its commercial use should be addressed to:

*Innovative Technology Assets Management
JPL*

*Mail Stop 321-123
4800 Oak Grove Drive
Pasadena, CA 91109-8099*

E-mail: iaoffice@jpl.nasa.gov

Refer to NPO-47655, volume and number of this NASA Tech Briefs issue, and the page number.

⚙️ Miga Aero Actuator and 2D Machined Mechanical Binary Latch

Applications include automobiles and deadbolts for windows or doors.

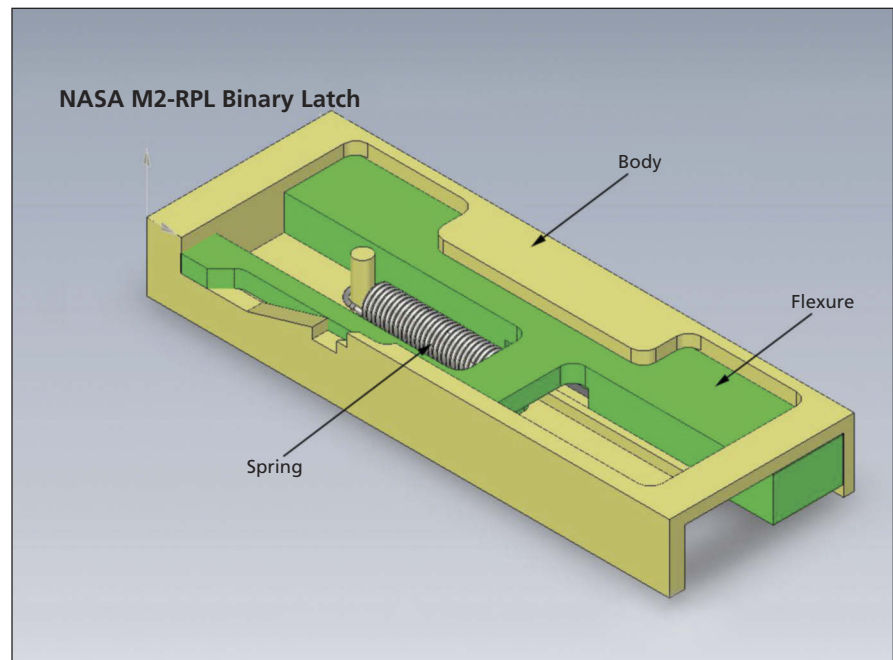
John H. Glenn Research Center, Cleveland, Ohio

Shape memory alloy (SMA) actuators provide the highest force-to-weight ratio of any known actuator. They can be designed for a wide variety of form factors from flat, thin packages, to form-matching packages for existing actuators. SMA actuators can be operated many thousands of times, so that ground testing is possible. Actuation speed can be accurately controlled from milliseconds to position and hold, and even electronic velocity-profile control is possible. SMA actuators provide a high degree of operational flexibility, and are truly smart actuators capable of being accurately controlled by onboard microprocessors across a wide range of voltages.

The Miga Aero actuator is a SMA actuator designed specifically for spaceflight applications. Providing 13 mm of stroke with either 20- or 40-N output force in two different models, the Aero actuator is made from low-outgassing PEEK (polyether ether ketone) plastic, stainless steel, and nickel-titanium SMA wires. The modular actuator weighs less than 28 grams. The dorsal output attachment allows the Aero to be used in either PUSH or PULL modes by inverting the mounting orientation.

The SPA1 actuator utilizes commercially available SMA actuator wire to provide 3/8-in. (≈ 1 cm) of stroke at a force of over 28 lb (≈ 125 N). The force is provided by a unique packaging of

the single SMA wire that provides the output force of four SMA wires mechanically in parallel. The output load is shared by allowing the SMA wire to “slip” around the output attachment



A model of the machined Mechanical Binary Latch.

end to adjust or balance the load, preventing any individual wire segment from experiencing high loads during actuation. A built-in end limit switch prevents overheating of the SMA element following actuation when used in conjunction with the Miga Analog Driver [a simple MOSFET (metal-oxide-semiconductor field-effect transistor) switching circuit].

A simple 2D machined mechanical binary latch has been developed to complement the capabilities of SMA wire actuators. SMA actuators typically perform ideally as “latch-release” devices, wherein a spring-loaded device is released when the SMA actuator actuates in one direction. But many applications require cycling between two latched states — open and closed.

This work was done by Mark A. Gummin of Miga Motor Company for NASA Glenn Research Center. Further information is contained in a TSP (see page 1).

Inquiries concerning rights for the commercial use of this invention should be addressed to NASA Glenn Research Center, Innovative Partnerships Office, Attn: Steven Fedor, Mail Stop 4-8, 21000 Brookpark Road, Cleveland, Ohio 44135. Refer to LEW-18582-1.



Micro-XRF for *In Situ* Geological Exploration of Other Planets

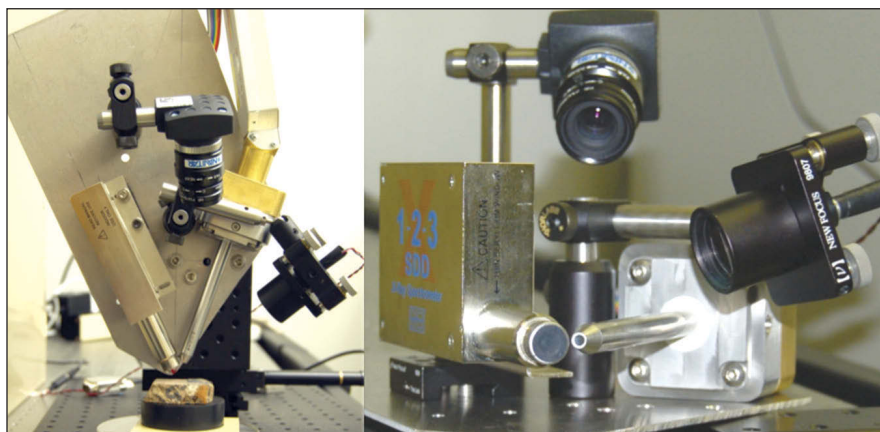
X-ray fluorescence instruments are used for non-destructive testing, sorting of recycled materials, and hazardous waste detection.

NASA's Jet Propulsion Laboratory, Pasadena, California

In situ analysis of rock chemistry is a fundamental tool for exploration of planets. To meet this need, a high-spatial-resolution micro x-ray fluorescence (Micro-XRF) instrument was developed that is capable of determining the elemental composition of rocks (elements Na–U) with 100 μm spatial resolution, thus providing insight to the composition of features as small as sand grains and individual laminae. The resulting excitation beam is of sufficient intensity that high signal-to-noise punctual spectra are acquired in seconds to a few minutes using an Amptek Silicon Drift Detector (SDD).

The instrument features a tightly focused x-ray tube and HVPS developed by Moxtek that provides up to 200 μA at 10 to 50 keV, with a custom polycapillary optic developed by XOS Inc. and integrated into a breadboard Micro-XRF (see figure). The total mass of the complete breadboard instrument is 2.76 kg, including mounting hardware, mounting plate, camera, laser, etc. A flight version of this instrument would require less than 5W nominal power and 1.5 kg mass.

The instrument includes an Amptek SDD that draws 2.5 W and has a resolu-



Two views of the breadboard **Micro-XRF Instrument**, which includes a Peltier-cooled detector with electronics, Moxtek HVPS, and x-ray tube integrated with an XOS polycapillary optic, a camera, and a focused laser.

tion of 135 to 155 eV FWHM at 5.9 keV. It weighs 180 g, including the preamplifier, digital pulse processor, multichannel analyzer, detector and preamp power supplies, and packaging. Rock samples are positioned relative to the instrument by a three-axis arm whose position is controlled by closed-loop translators (mimicking the robotic arm of a rover). The distance from the source to the detector is calculated from the position of a focused laser beam on the sam-

ple as imaged by the camera. The instrument enables quick scans of major elements in only 1 second, and rapid acquisition (30 s) of data with excellent signal-to-noise and energy resolution for trace element analysis.

This work was done by Lawrence A. Wade, Robert P. Hodyss, and Abigail C. Allwood of Caltech; Ning Gao of XOS; and Kris Kozaczek of Moxtek for NASA's Jet Propulsion Laboratory. Further information is contained in a TSP (see page 1). NPO-48599

Hydrogen-Enhanced Lunar Oxygen Extraction and Storage Using Only Solar Power

Oxygen-generating concept can be developed in an efficient system with low specific mass.

Marshall Space Flight Center, Alabama

The innovation consists of a thermodynamic system for extracting *in situ* oxygen vapor from lunar regolith using a solar photovoltaic power source in a reactor, a method for thermally insulating the reactor, a method for protecting the reactor internal components from oxidation by the extracted oxygen, a method for removing unwanted chemical species produced in the reactor from

the oxygen vapor, a method for passively storing the oxygen, and a method for releasing high-purity oxygen from storage for lunar use.

Lunar oxygen exists in various types of minerals, mostly silicates. The energy required to extract the oxygen from the minerals is 30 to 60 MJ/kg O. Using simple heating, the extraction rate depends on temperature. The

minimum temperature is approximately 2,500 K, which is at the upper end of available oven temperatures. The oxygen is released from storage in a purified state, as needed, especially if for human consumption.

This method extracts oxygen from regolith by treating the problem as a closed batch cycle system. The innovation works equally well in Earth or Lunar

gravity fields, at low partial pressure of oxygen, and makes use of *in situ* regolith for system insulation.

The innovation extracts oxygen from lunar regolith using a method similar to vacuum pyrolysis, but with hydrogen cover gas added stoichiometrically to react with the oxygen as it is produced by radiatively heating regolith to 2,500 K. The hydrogen flows over and through the heating element (HE), protecting it from released oxygen. The H₂-O₂ heat of reaction is regeneratively recovered to assist the heating process. Lunar regolith is loaded into a large-diameter, low-height “pancake” reactor powered by photovoltaic cells. The reactor lid contains a 2,500 K HE that radiates

downward onto the regolith to heat it and extract oxygen, and is shielded above by a multi-layer tungsten radiation shield. Hydrogen cover gas percolates through the perforated tungsten shielding and HE, preventing oxidation of the shielding and HE, and reacting with the oxygen to form water vapor. The water vapor is filtered through solid regolith to remove unwanted extraction byproducts, and then condensed to a liquid state and stored at 300 to 325 K. Conversion to usable oxygen is achieved by pumping liquid water into a high-pressure electrolyzer, storing the gaseous oxygen at high pressure for use, and diverting the hydrogen back to the reactor or to storage.

The results from this design effort show that this oxygen-generating concept can be developed in an efficient system with low specific mass. Advantages include use of regolith as an oxygen source, filter, and thermal insulator. The system can be tested in Earth gravity and can be expected to operate similarly in lunar gravity. The system is scalable, either by increasing the power level and output of a standard module, or by employing multiple modules.

This work was done by Rodney Burton and Darren King of CU Aerospace LLC for Marshall Space Flight Center. For more information, contact Sammy Nabors, MSFC Commercialization Assistance Lead, at sammy.a.nabors@nasa.gov. Refer to MFS-32933-1.

Uplift of Ionospheric Oxygen Ions During Extreme Magnetic Storms

NASA's Jet Propulsion Laboratory, Pasadena, California

Research reported earlier in literature was conducted relating to estimation of the ionospheric electrical field, which may have occurred during the September 1859 Carrington geomagnetic storm event, with regard to modern-day consequences.

In this research, the NRL SAMI2 ionospheric code has been modified and applied the estimated electric field to the dayside ionosphere. The modeling was done at 15-minute time increments to

track the general ionospheric changes. Although it has been known that magnetospheric electric fields get down into the ionosphere, it has been only in the last ten years that scientists have discovered that intense magnetic storm electric fields do also. On the dayside, these dawn-to-dusk directed electric fields lift the plasma (electrons and ions) up to higher altitudes and latitudes. As plasma is removed from lower altitudes, solar UV creates new plasma, so the total plasma in the ionosphere is increased several-fold. Thus, this complex process creates super-dense plasmas at high altitudes (from 700 to 1,000 km and higher).

This work was done by Bruce T. Tsurutani, Anthony J. Mannucci, and Olga P. Verkhotyadova of Caltech; Joseph Huba of Naval Research Laboratory; and Gurbax S. Lakhina of the Indian Institute of Geomagnetism for NASA's Jet Propulsion Laboratory. For more information, contact iaoffice@jpl.nasa.gov. NPO-48762

Miniaturized, High-Speed, Modulated X-Ray Source

An extremely robust photon-driven electron source is used that can tolerate weeks or more of exposure to air.

Goddard Space Flight Center, Greenbelt, Maryland

A low-cost, miniature x-ray source has been developed that can be modulated in intensity from completely off to full intensity on nanosecond timescales. This modulated x-ray source (MXS) has no filaments and is extremely rugged. The energy level of the MXS is adjustable from 0 to more than 100 keV. It can be used as the core of many new devices, providing the first practical, arbitrarily time-variable source of x-rays. The high-speed switching capability and miniature size make possible many new technologies including x-ray-based communication, compact time-resolved x-

ray diffraction, novel x-ray fluorescence instruments, and low- and precise-dose medical x-rays.

To make x-rays, the usual method is to accelerate electrons into a target material held at a high potential. When the electrons stop in the target, x-rays are produced with a spectrum that is a function of the target material and the energy to which the electrons are accelerated. Most commonly, the electrons come from a hot filament. In the MXS, the electrons start off as optically driven photoelectrons. The modulation of the x-rays is then tied to the modulation of the light

that drives the photoelectron source. Much of the recent development has consisted of creating a photoelectrically-driven electron source that is robust, low in cost, and offers high intensity.

For robustness, metal photocathodes were adopted, including aluminum and magnesium. Ultraviolet light from 255- to 350-nm LEDs (light emitting diodes) stimulated the photoemissions from these photocathodes with an efficiency that is maximized at the low-wavelength end (255 nm) to a value of roughly 10⁻⁴. The MXS units now have much higher brightness, are much smaller,

and are made using a number of commercially available components, making them extremely inexpensive.

In the latest MXS design, UV efficiency is addressed by using a high-gain electron multiplier. The photocathode is vapor-deposited onto the input cone of a Burle Magnum™ multiplier. This system

yields an extremely robust photon-driven electron source that can tolerate long — weeks or more — exposure to air with negligible degradation. The package is also small. When combined with the electron target, necessary vacuum fittings, and supporting components (but not including LED electron-

ics or high-voltage sources), the entire modulated x-ray source weighs as little as 158 grams.

This work was done by Keith Gendreau, Zaven Arzoumanian, Steve Kenyon, and Nick Spartana of Goddard Space Flight Center. Further information is contained in a TSP (see page 1). GSC-16287-1

Hollow-Fiber Spacesuit Water Membrane Evaporator

Commercial applications include personal coolers for infantry, humidifiers for pilots, and personal coolers for hazmat suits.

Lyndon B. Johnson Space Center, Houston, Texas

The hollow-fiber spacesuit water membrane evaporator (HoFi SWME) is being developed to perform the thermal control function for advanced spacesuits and spacecraft to take advantage of recent advances in micropore membrane technology in providing a robust, heat-rejection device that is less sensitive to contamination than is the sublimator. After recent contamination tests, a commercial-off-the-shelf (COTS) microporous hollow-fiber membrane was selected for prototype development as the most suitable candidate among commercial hollow-fiber evaporator alternatives. An innovative design that grouped the fiber layers into stacks,

which were separated by small spaces and packaged into a cylindrical shape, was developed into a full-scale prototype for the spacesuit application.

Vacuum chamber testing has been performed to characterize heat rejection as a function of inlet water temperature and water vapor backpressure, and to show contamination resistance to the constituents expected to be found in potable water produced by the wastewater reclamation distillation processes. Other tests showed tolerance to freezing and suitability to reject heat in a Mars pressure environment. In summary, HoFi SWME is a lightweight, compact evaporator for heat rejection

in the spacesuit that is robust, contamination-insensitive, freeze-tolerant, and able to reject the required heat of spacewalks in microgravity, lunar, and Martian environments.

The HoFi is packaged to reject 810 W of heat through 800 hours of use in a vacuum environment, and 370 W in a Mars environment. The device also eliminates free gas and dissolved gas from the coolant loop.

This work was done by Grant Bue and Luis Trevino of Johnson Space Center; Gus Tsioulos of Wyle; Keith Mitchell of Jacobs Technology, Inc.; and Joseph Settles of Barrios. Further information is contained in a TSP (see page 1). MSC-24849-1

High-Power Single-Mode 2.65- μm InGaAsSb/AlInGaAsSb Diode Lasers

This innovation is useful for targeted gas detection instruments in environmental monitoring, safety, quality control, and fundamental science applications.

NASA's Jet Propulsion Laboratory, Pasadena, California

Central to the advancement of both satellite and in-situ science are improvements in continuous-wave and pulsed infrared laser systems coupled with integrated miniaturized optics and electronics, allowing for the use of powerful, single-mode light sources aboard both satellite and unmanned aerial vehicle platforms.

There is a technological gap in supplying adequate laser sources to address the mid-infrared spectral window for spectroscopic characterization of important atmospheric gases. For high-power applications between 2 to 3 μm , commercial laser technologies are unsuitable because of limitations in output power. For

instance, existing InP-based laser systems developed for fiber-based telecommunications cannot be extended to wavelengths longer than 2 μm . For emission wavelengths shorter than 3 μm , intersubband devices, such as infrared quantum cascade lasers, become inefficient due to band-offset limitations. To date, successfully demonstrated single-mode GaSb-based laser diodes emitting between 2 and 3 μm have employed lossy metal Bragg gratings for distributed-feedback coupling, which limits output power due to optical absorption.

By optimizing both the quantum well design and the grating fabrication process, index-coupled distributed-feed-

back 2.65- μm lasers capable of emitting in excess of 25 mW at room temperature have been demonstrated. Specifically, lasers at 3,777 cm^{-1} (2.65 μm) have been realized to interact with strong absorption lines of HDO and other isotopologues of H₂O. With minor modifications of the optical cavity and quantum well designs, lasers can be fabricated at any wavelength within the 2-to-3- μm spectral window with similar performance. At the time of this reporting, lasers with this output power and wavelength accuracy are not commercially available.

Monolithic ridge-waveguide GaSb lasers were fabricated that utilize second-order lateral Bragg gratings to generate

single-mode emission from InGaAsSb/AlInGaAsSb multi-quantum well structures. The device fabrication utilizes etched index-coupled gratings in the top AlGaAsSb cladding of the laser chip along the ridge waveguide, whereas commercial lasers that emit close to this wavelength include loss-coupled metal gratings that limit the output power of the laser.

Semiconductor-laser-based spectrometers can be used to replace gas sensors currently used in industry and govern-

ment. With the availability of high-power laser sources at mid-infrared wavelengths, sensors can target strong fundamental gas absorption lines to maximize instrument sensitivity.

This work was done by Clifford F. Frez, Ryan M. Briggs, Siamak Forouhar, and Carl E. Borgentun of Caltech; and James Gupta of the National Research Council, Canada for NASA's Jet Propulsion Laboratory. For more information, contact iaoffice@jpl.nasa.gov.

In accordance with Public Law 96-517,

the contractor has elected to retain title to this invention. Inquiries concerning rights for its commercial use should be addressed to:

*Innovative Technology Assets Management
JPL*

*Mail Stop 321-123
4800 Oak Grove Drive
Pasadena, CA 91109-8099*

E-mail: iaoffice@jpl.nasa.gov

Refer to NPO-48926, volume and number of this NASA Tech Briefs issue, and the page number.

Optical Device for Converting a Laser Beam Into Two Co-aligned but Oppositely Directed Beams

Goddard Space Flight Center, Greenbelt, Maryland

Optical systems consisting of a series of optical elements require alignment from the input end to the output end. The optical elements can be mirrors, lenses, sources, detectors, or other devices. Complex optical systems are often difficult to align from end-to-end because the alignment beam must be inserted at one end in order for the beam to traverse the entire optical path to the other end. The ends of the optical train may not be easily accessible to the alignment beam.

Typically, when a series of optical elements is to be aligned, an alignment laser beam is inserted into the optical path with a pick-off mirror at one end of the series of elements. But it may be impossible to insert the beam at an end-

point. It can be difficult to locate the pick-off mirror at the desired position because there is not enough space, there is no mounting surface, or the location is occupied by a source, detector, or other component. Alternatively, the laser beam might be inserted at an intermediate location (not at an end-point) and sent, first in one direction and then the other, to the opposite ends of the optical system for alignment. However, in this case, alignment must be performed in two directions and extra effort is required to co-align the two beams to make them parallel and coincident, i.e., to follow the same path as an end-to-end beam.

An optical device has been developed that accepts a laser beam as input and produces two co-aligned, but counter-

propagating beams. In contrast to a conventional alignment laser placed at one end of the optical path, this invention can be placed at a convenient position within the optical train and aligned to send its two beams simultaneously along precisely opposite paths that, taken together, trace out exactly the same path as the conventional alignment laser. This invention allows the user the freedom to choose locations within the optical train for placement of the alignment beam. It is also self-aligned by design and requires almost no adjustment.

This work was done by Donald Jennings of Goddard Space Flight Center. Further information is contained in a TSP (see page 1). GSC-16610-1

A Hybrid Fiber/Solid-State Regenerative Amplifier with Tunable Pulse Widths for Satellite Laser Ranging

Applications include materials processing, remote detection, and high-resolution 3D image mapping.

Goddard Space Flight Center, Greenbelt, Maryland

A fiber/solid-state hybrid seeded regenerative amplifier, capable of achieving high output energy with tunable pulse widths, has been developed for satellite laser ranging applications. The regenerative amplifier cavity uses a pair of Nd:YAG zigzag slabs oriented orthogonally to one another in order to make thermal lensing effects symmetrical and simplify optical correction schemes. The seed laser used is a fiber-coupled 1,064-nm narrowband

(<0.02 nm) diode laser that is discretely driven in a new short-pulsed mode, enabling continuously tunable seed pulse widths in the 0.2-to-0.4-ns range.

The amplifier gain unit consists of a pair of Brewster-cut 6-bounce zigzag Nd:YAG laser slabs, oriented 90° relative to each other in the amplifier head. This arrangement creates a net-symmetrical thermal lens effect (an opposing single-axis effect in each slab), and makes

thermo-optical corrections simple by optimizing the curvature of the nearest cavity mirror. Each slab is pumped by a single 120-W, pulsed 808-nm laser diode array. In this configuration, the average pump beam distribution in the slabs had a 1-D Gaussian shape, which matches the estimated cavity mode size. A half-wave plate between the slabs reduces losses from Fresnel reflections due to the orthogonal slabs' Brewster-cut end faces.

Successful “temporal” seeding of the regenerative amplifier cavity results in a cavity Q-switch pulse envelope segmenting into shorter pulses, each having the width of the input seed, and having a uniform temporal separation corresponding to the cavity round-trip time of ≈ 10 ns. The pulse energy is allowed to build on successive passes in the regenerative amplifier cavity until a maximum is reached, (when cavity gains and losses are equal), after which the pulse is electro-optically switched out on the next round trip.

The overall gain of the amplifier is ≈ 82 dB (or a factor of 1.26 million). After directing the amplified output through a LBO frequency doubling crys-

tal, ≈ 2.1 W of 532-nm output (>1 mJ) was measured. This corresponds to a nonlinear conversion efficiency of $>60\%$. Furthermore, by pulse pumping this system, a single pulse per laser shot can be created for the SLR (satellite laser ranging) measurement, and this can be ejected into the instrument. This is operated at the precise frequency needed by the measurement, as opposed to commercial short-pulsed, mode-locked systems that need to operate in a continuous fashion, or CW (continuous wave), and create pulses at many MHz. Therefore, this design does not need to “throw away” or dump 99% of the laser energy to produce what is required; this system can be far smaller, more efficient,

cheaper, and readily deployed in the field when packaged efficiently.

Finally, by producing custom diode seed pulses electronically, two major advantages over commercial systems are realized: First, this pulse shape is customizable and not affected by the cavity length or gain of the amplifier cavity, and second, it can produce adjustable (selectable) pulse widths by simply adding multiple seed diodes and coupling each into commercial, low-cost fiber-optic combiners.

This work was done by Barry Coyle of Goddard Space Flight Center and Demetrios Poullos of American University. Further information is contained in a TSP (see page 1). GSC-16550-1

X-Ray Diffractive Optics

Goddard Space Flight Center, Greenbelt, Maryland

X-ray optics were fabricated with the capability of imaging solar x-ray sources with better than 0.1 arcsecond angular resolution, over an order of magnitude finer than is currently possible.

Such images would provide a new window into the little-understood energy release and particle acceleration regions in solar flares. They constitute one of the most promising ways to probe these regions in the solar atmosphere with the sensitivity and angular resolution

needed to better understand the physical processes involved.

A circular slit structure with widths as fine as 0.85 micron etched in a silicon wafer 8 microns thick forms a phase zone plate version of a Fresnel lens capable of focusing ≈ 6 keV x-rays. The focal length of the 3-cm diameter lenses is 100 m, and the angular resolution capability is better than 0.1 arcsecond. Such phase zone plates were fabricated in Goddard’s Detector Development Lab. (DDL) and

tested at the Goddard 600-m x-ray test facility. The test data verified that the desired angular resolution and throughput efficiency were achieved.

This work was done by Brian Dennis and Mary Li of Goddard Space Flight Center and Gerald Skinner of the University of Maryland. For further information, contact the Goddard Innovative Partnerships Office at (301) 286-5810. GSC-16418-1



➤ SynGenics Optimization System (SynOptSys)

The SynGenics Optimization System (SynOptSys) software application optimizes a product with respect to multiple, competing criteria using statistical Design of Experiments, Response-Surface Methodology, and the Desirability Optimization Methodology. The user is not required to be skilled in the underlying math; thus, SynOptSys can help designers and product developers overcome the barriers that prevent them from using powerful techniques to develop better products in a less costly manner. SynOptSys is applicable to the design of any product or process with multiple criteria to meet, and at least two factors that influence achievement of those criteria.

The user begins with a selected solution principle or system concept and a set of criteria that needs to be satisfied. The criteria may be expressed in terms of documented desirabilities or defined responses that the future system needs to achieve. Documented desirabilities can be imported into SynOptSys or created and documented directly within SynOptSys. Subsequent steps include identifying factors, specifying model order for each response, designing the experiment, running the experiment and gathering the data, analyzing the results, and determining the specifications for the optimized system. The user may also enter textual information as the project progresses. Data is easily edited within SynOptSys, and the software design enables full traceability within any step in the process, and facilitates reporting as needed.

SynOptSys is unique in the way responses are defined and the nuances of the goodness associated with changes in response values for each of the responses of interest. The Desirability Optimization Methodology provides the basis of this novel feature. Moreover, this is a complete, guided design and optimization process tool with embedded math that can remain invisible to the user. It is not a standalone statistical program; it is a design and optimization system.

This work was done by Carol Ventresca, Michelle L. McMillan, and Stephanie Globus of SynGenics Corporation for Glenn Research Center. Further information is contained in a TSP (see page 1).

Inquiries concerning rights for the commercial use of this invention should be addressed to NASA Glenn Research Center, Innovative Partnerships Office, Attn: Steven Fedor, Mail Stop 4-8, 21000 Brookpark Road, Cleveland, Ohio 44135. Refer to LEW-18924-1.

➤ CFD Script for Rapid TPS Damage Assessment

This grid generation script creates unstructured CFD grids for rapid thermal protection system (TPS) damage aeroheating assessments. The existing manual solution is cumbersome, open to errors, and slow.

The invention takes a large-scale geometry grid and its large-scale CFD solution, and creates a unstructured “patch” grid that models the TPS damage. The flow field boundary condition for the “patch” grid is then interpolated from the large-scale CFD solution. It speeds up the generation of CFD grids and solutions in the modeling of TPS damages and their aeroheating assessment. This process was successfully utilized during STS-134.

This work was done by Peter McCloud of The Boeing Company for Johnson Space Center. For further information, contact the JSC Innovation Partnerships Office at (281) 483-3809. MSC-24865-1

➤ radEq Add-On Module for CFD Solver Loci-CHEM

The radEq software module allows Loci-CHEM to be applied to flow velocities where surface radiation due to heating from compression and friction becomes significant. The module adds a radiation equilibrium boundary condition to the computational fluid dynamics (CFD) code to produce accurate results. The module expanded the upper limit for accurate CFD solutions of Loci-CHEM from Mach 4 to Mach 10 based on Space Shuttle Orbiter Re-Entry trajectories.

Loci-CHEM already has a very promising architecture and performance, but absence of radiation equilibrium boundary condition limited the application of Loci-CHEM to below Mach 4. The immediate advantage of the add-on module is that it allows Loci-CHEM to work with supersonic flows up to Mach 10. This transformed Loci-CHEM from a rocket engine-heritage CFD code with general

subsonic and low-supersonic applications, to an aeroheating code with hypersonic applications. The follow-on advantage of the module is that it is a building block for additional add-on modules that will solve for the heating generated at Mach numbers higher than 10.

This work was done by Peter McCloud of The Boeing Company. For further information, contact the JSC Innovation Partnerships Office at (281) 483-3809.

Title to this invention has been waived under the provisions of the National Aeronautics and Space Act {42 U.S.C. 2457(f)} to The Boeing Company. Inquiries concerning licenses for its commercial development should be addressed to:

*The Boeing Company
2201 Seal Beach Boulevard
P.O. Box 2515
Seal Beach, CA 90740-1515*

Refer to MSC-24848-1, volume and number of this NASA Tech Briefs issue, and the page number.

➤ Science Opportunity Analyzer (SOA) Version 8

SOA allows scientists to plan spacecraft observations. It facilitates the identification of geometrically interesting times in a spacecraft’s orbit that a user can use to plan observations or instrument-driven spacecraft maneuvers. These observations can then be visualized multiple ways in both two- and three-dimensional views. When observations have been optimized within a spacecraft’s flight rules, the resulting plans can be output for use by other JPL uplink tools. Now in its eighth major version, SOA improves on these capabilities in a modern and integrated fashion.

SOA consists of five major functions: Opportunity Search, Visualization, Observation Design, Constraint Checking, and Data Output. Opportunity Search is a GUI-driven interface to existing search engines that can be used to identify times when a spacecraft is in a specific geometrical relationship with other bodies in the solar system. This function can be used for advanced mission planning as well as for making last-minute adjustments to mission sequences in response to trajectory modifications. Visualization is a key aspect of SOA. The user can view observation opportunities in either a 3D representation or as a 2D map projection.

Observation Design allows the user to orient the spacecraft and visualize the projection of the instrument field of view for that orientation using the same views as Opportunity Search. Constraint Checking is provided to validate various geometrical and physical aspects of an observation design. The user has the ability to easily create custom rules or to use official project-generated flight rules. This capability may also allow scientists to easily assess the cost to science if flight rule changes occur. Data Output allows the user to compute ancillary data related to an observation or to a given position of the spacecraft along its trajectory. The data can be saved as a tab-delimited text file or viewed as a graph.

SOA combines science planning functionality unique to both JPL and the sponsoring spacecraft. SOA is able to ingest JPL SPICE Kernels that are used to drive the tool and its computations. A Percy search engine is then included that identifies interesting time periods for the user to build observations. When observations are then built, flight-like orientation algorithms replicate spacecraft dynamics to closely simulate the flight spacecraft's dynamics.

SOA v8 represents large steps forward from SOA v7 in terms of quality, reliability, maintainability, efficiency, and user experience. A tailored agile development environment has been built around SOA that provides automated unit testing, continuous build and integration, a con-

solidated Web-based code and documentation storage environment, modern Java enhancements, and a focus on usability.

This work was done by Robert J. Witoff, Carol A. Polanskey, Anna Marie A. Aguinaldo, Ning Liu, and Mark D. Hofstadler of Caltech; and Steven P. Joy of UCLA for NASA's Jet Propulsion Laboratory. For more information, contact iaoffice@jpl.nasa.gov.

This software is available for commercial licensing. Please contact Dan Broderick at Daniel.F.Broderick@jpl.nasa.gov. Refer to NPO-48529.

Autonomous Byte Stream Randomizer

Net-centric networking environments are often faced with limited resources and must utilize bandwidth as efficiently as possible. In networking environments that span wide areas, the data transmission has to be efficient without any redundant or exuberant metadata.

The Autonomous Byte Stream Randomizer software provides an extra level of security on top of existing data encryption methods. Randomizing the data's byte stream adds an extra layer to existing data protection methods, thus making it harder for an attacker to decrypt protected data. Based on a generated cryptographically secure random seed, a random sequence of numbers is used to intelligently and efficiently swap the organization of bytes in data using the unbiased and memory-efficient in-place Fisher-Yates shuffle method.

Swapping bytes and reorganizing the crucial structure of the byte data renders the data file unreadable and leaves the data in a deconstructed state. This deconstruction adds an extra level of security requiring the byte stream to be reconstructed with the random seed in order to be readable. Once the data byte stream has been randomized, the software enables the data to be distributed to N nodes in an environment. Each piece of the data in randomized and distributed form is a separate entity unreadable on its own right, but when combined with all N pieces, is able to be reconstructed back to one.

Reconstruction requires possession of the key used for randomizing the bytes, leading to the generation of the same cryptographically secure random sequence of numbers used to randomize the data. This software is a cornerstone capability possessing the ability to generate the same cryptographically secure sequence on different machines and time intervals, thus allowing this software to be used more heavily in net-centric environments where data transfer bandwidth is limited.

This work was done by George K. Paloulian, Simon S. Woo, and Edward T. Chow of Caltech for NASA's Jet Propulsion Laboratory. Further information is contained in a TSP (see page 1).

This software is available for commercial licensing. Please contact Dan Broderick at Daniel.F.Broderick@jpl.nasa.gov. Refer to NPO-48495.



➤ Distributed Engine Control Empirical/Analytical Verification Tools

Key factors such as control system performance, reliability, weight, and bandwidth utilization can be systematically assessed.

John H. Glenn Research Center, Cleveland, Ohio

NASA's vision for an intelligent engine will be realized with the development of a truly distributed control system featuring highly reliable, modular, and dependable components capable of both surviving the harsh engine operating environment and decentralized functionality. A set of control system verification tools was developed and applied to a C-MAPSS40K engine model, and metrics were established to assess the stability and performance of these control systems on the same platform. A software tool was developed that allows designers to assemble easily a distributed control system in software and immediately assess the overall impacts of the system on the target (simulated) platform, allowing control system designers to converge rapidly on acceptable architectures with consideration to all required hardware elements. The software developed in this program will be installed on a distributed hardware-in-the-loop (DHIL) simulation tool to assist NASA and the Distributed Engine Control Working Group (DECWG) in integrating DCS (distributed engine control systems) components onto existing and next-generation engines.

The distributed engine control simulator blockset for MATLAB/Simulink and hardware simulator provides the capability to simulate "virtual" subcomponents, as well as swap actual subcomponents for hardware-in-the-loop (HIL) analysis. Subcomponents can be the communication network, smart sensor or actuator nodes, or a centralized control system. The distributed engine control blockset for MATLAB/Simulink is a software development tool. The software includes an engine simulation, a communication network simulation, control algorithms, and analysis algorithms set up in a modular environment for rapid simulation of different network architectures; the hardware consists of an embedded device running parts of the C-MAPSS engine simulator and controlled through Simulink.

The distributed engine control simulation, evaluation, and analysis technology provides unique capabilities to study the effects of a given change to the control system in the context of the distributed paradigm. The simulation tool can support treatment of all components within the control system, both "virtual" and real; these include communication data network, smart sensor

and actuator nodes, centralized control system (FADEC — full authority digital engine control), and the aircraft engine itself. The DECsim tool can allow simulation-based prototyping of control laws, control architectures, and decentralization strategies before hardware is integrated into the system. With the configuration specified, the simulator allows a variety of key factors to be systematically assessed. Such factors include control system performance, reliability, weight, and bandwidth utilization. The ability to provide a configurable, high-fidelity distributed engine control simulation, control system analysis, and HIL evaluation is a unique capability of the technology.

This work was done by Jonathan DeCastro and Eric Hettler of Impact Technologies, LLC; Rama Yedavalli of the Ohio State University; and Sayan Mitra of the University of Illinois at Urbana for Glenn Research Center. Further information is contained in a TSP (see page 1).

Inquiries concerning rights for the commercial use of this invention should be addressed to NASA Glenn Research Center, Innovative Partnerships Office, Attn: Steven Fedor, Mail Stop 4-8, 21000 Brookpark Road, Cleveland, Ohio 44135. Refer to LEW-18829-1.

➤ Dynamic Server-Based KML Code Generator Method for Level-of-Detail Traversal of Geospatial Data

Innovation uses a C- or PHP-code-like grammar that provides a high degree of processing flexibility.

Stennis Space Center, Mississippi

Geospatial data servers that support Web-based geospatial client applications such as Google Earth and NASA World Wind must listen to data requests, access appropriate stored data, and compile a data response to the requesting client application. This process occurs repeatedly to support multiple client requests and application instances. Newer Web-based

geospatial clients also provide user-interactive functionality that is dependent on fast and efficient server responses. With massively large datasets, server-client interaction can become severely impeded because the server must determine the best way to assemble data to meet the client applications request. In client applications such as Google Earth, the user

interactively wanders through the data using visually guided panning and zooming actions. With these actions, the client application is continually issuing data requests to the server without knowledge of the server's data structure or extraction/assembly paradigm.

A method for efficiently controlling the networked access of a Web-based

geospatial browser to server-based datasets — in particular, massively sized datasets — has been developed. The method specifically uses the Keyhole Markup Language (KML), an Open Geospatial Consortium (OGS) standard used by Google Earth and other KML-compliant geospatial client applications. The innovation is based on establishing a dynamic cascading KML strategy that is initiated by a KML launch file provided by a data server host to a Google Earth or similar KML-compliant geospatial client application user. Upon execution, the launch KML code issues a request for image data covering an initial geographic region. The server responds with the requested data along with subsequent dynamically generated KML code that directs the client application to make follow-

on requests for higher level of detail (LOD) imagery to replace the initial imagery as the user navigates into the dataset. The approach provides an efficient data traversal path and mechanism that can be flexibly established for any dataset regardless of size or other characteristics. The method yields significant improvements in user-interactive geospatial client and data server interaction and associated network bandwidth requirements.

The innovation uses a C- or PHP-code-like grammar that provides a high degree of processing flexibility. A set of language lexer and parser elements is provided that offers a complete language grammar for writing and executing language directives. A script is wrapped and passed to the geospatial data server by a client application as a

component of a standard KML-compliant statement. The approach provides an efficient means for a geospatial client application to request server preprocessing of data prior to client delivery.

Data is structured in a quadtree format. As the user zooms into the dataset, geographic regions are subdivided into four child regions. Conversely, as the user zooms out, four child regions collapse into a single, lower-LOD region. The approach provides an efficient data traversal path and mechanism that can be flexibly established for any dataset regardless of size or other characteristics.

This work was done by Gregory Baxes, Brian Mixon, and Tim Linger of TerraMetrics, Inc. for Stennis Space Center. For more information call the SSC Center Chief Technologist at (228) 688-1929. Refer to SSC-00362/5.

Automated Planning of Science Products Based on Nadir Overflights and Alerts for Onboard and Ground Processing

NASA's Jet Propulsion Laboratory, Pasadena, California

A set of automated planning algorithms is the current operations baseline approach for the Intelligent Payload Module (IPM) of the proposed Hyperspectral Infrared Imager (HyspIRI) mission. For this operations concept, there are only local (e.g. non-depletable) operations constraints, such as real-time downlink and onboard memory, and the forward sweeping algorithm is optimal for determining which science products should be generated onboard and on ground based on geographical overflights, science priorities, alerts, requests, and onboard and ground processing constraints.

This automated planning approach was developed for the HyspIRI IPM

concept. The HyspIRI IPM is proposed to use an X-band Direct Broadcast (DB) capability that would enable data to be delivered to ground stations virtually as it is acquired. However, the HyspIRI VSWIR and TIR instruments will produce approximately 1 Gbps data, while the DB capability is 15 Mbps for a $\approx 60\times$ oversubscription. In order to address this mismatch, this innovation determines which data to downlink based on both the type of surface the spacecraft is overflying, and the onboard processing of data to detect events. For example, when the spacecraft is overflying Polar Regions, it might downlink a snow/ice product.

Additionally, the onboard software will search for thermal signatures indicative of a volcanic event or wild fire and downlink summary information (extent, spectra) when detected, thereby reducing data volume. The planning system described above automatically generated the IPM mission plan based on requested products, the overflight regions, and available resources.

This work was done by Steve A. Chien, David A. McLaren, and Gregg R. Rabideau of Caltech; Daniel Mandl of NASA Goddard Space Flight Center; and Jerry Hengemihle of Microtel LLC for NASA's Jet Propulsion Laboratory. Further information is contained in a TSP (see page 1). NPO-47875

Linked Autonomous Interplanetary Satellite Orbit Navigation

Single satellite can track another satellite elsewhere in the Earth-Moon system and obtain absolute knowledge of both satellites' states.

NASA's Jet Propulsion Laboratory, Pasadena, California

A navigation technology known as LI-AISON (Linked Autonomous Interplanetary Satellite Orbit Navigation) has been known to produce very impressive navigation results for scenarios involving two or more cooperative satellites near the Moon, such that at least

one satellite must be in an orbit significantly perturbed by the Earth, such as a lunar halo orbit. The two (or more) satellites track each other using satellite-to-satellite range and/or range-rate measurements. These relative measurements yield absolute orbit navigation

when one of the satellites is in a lunar halo orbit, or the like.

The geometry between a lunar halo orbiter and a GEO satellite continuously changes, which dramatically improves the information content of a satellite-to-satellite tracking signal. The

geometrical variations include significant out-of-plane shifts, as well as in-plane shifts. Further, the GEO satellite is almost continuously in view of a lunar halo orbiter. High-fidelity simulations demonstrate that LiAISON technology improves the navigation of GEO orbiters by an order of magnitude, relative to standard ground tracking. If a GEO satellite is navigated using LiAISON-only tracking measurements, its position is typically known to better than 10 meters. If LiAISON measurements are combined with simple radiometric ground observations, then the satellite's position is typically known to better than 3 meters, which is substantially better than the current state of GEO navigation.

There are two features of LiAISON that are novel and advantageous compared with conventional satellite navigation. First, ordinary satellite-to-satellite tracking data only provides relative navigation of each satellite. The novelty is the placement of one navigation satellite in an orbit that is significantly perturbed by both the Earth and the Moon. A navigation satellite can track other satellites elsewhere in the Earth-Moon system and acquire knowledge about both satellites' absolute positions and velocities, as well as relative positions and velocities in space.

The second novelty is that ordinarily one requires many satellites in order to achieve full navigation of any given customer's position and velocity over time.

With LiAISON navigation, only a single navigation satellite is needed, provided that the satellite is significantly affected by the gravity of the Earth and the Moon. That single satellite can track another satellite elsewhere in the Earth-Moon system and obtain absolute knowledge of both satellites' states.

This work was done by Jeffrey S. Parker and Rodney L. Anderson of Caltech; and George H. Born, Jason M. Leonard, Ryan M. McGranaghan, and Kohei Fujimoto of the University of Colorado at Boulder for NASA's Jet Propulsion Laboratory. Further information is contained in a TSP (see page 1).

The software used in this innovation is available for commercial licensing. Please contact Dan Broderick at Daniel.F.Broderick@jpl.nasa.gov. Refer to NPO-48736.

➤ Risk-Constrained Dynamic Programming for Optimal Mars Entry, Descent, and Landing

NASA's Jet Propulsion Laboratory, Pasadena, California

A chance-constrained dynamic programming algorithm was developed that is capable of making optimal sequential decisions within a user-specified risk bound. This work handles stochastic uncertainties over multiple stages in the CEMAT (Combined EDL-Mobility Analyses Tool) framework. It was demonstrated by a simulation of Mars entry, descent, and landing (EDL) using real landscape data obtained from the Mars Reconnaissance Orbiter.

Although standard dynamic programming (DP) provides a general frame-

work for optimal sequential decision-making under uncertainty, it typically achieves risk aversion by imposing an arbitrary penalty on failure states. Such a penalty-based approach cannot explicitly bound the probability of mission failure. A key idea behind the new approach is called risk allocation, which decomposes a joint chance constraint into a set of individual chance constraints and distributes risk over them. The joint chance constraint was reformulated into a constraint on an expecta-

tion over a sum of an indicator function, which can be incorporated into the cost function by dualizing the optimization problem. As a result, the chance-constraint optimization problem can be turned into an unconstrained optimization over a Lagrangian, which can be solved efficiently using a standard DP approach.

This work was done by Masahiro Ono and Yoshiaki Kuwata of Caltech for NASA's Jet Propulsion Laboratory. For more information, contact iaoffice@jpl.nasa.gov. NPO-48606

➤ Scheduling Operations for Massive Heterogeneous Clusters

Goddard Space Flight Center, Greenbelt, Maryland

High-performance computing (HPC) programming has become increasingly difficult with the advent of hybrid supercomputers consisting of multicore CPUs and accelerator boards such as the GPU. Manual tuning of software to achieve high performance on this type of machine has been performed by programmers. This is needlessly difficult and prone to being invalidated by new hardware, new software, or changes in the underlying code.

A system was developed for task-based representation of programs, which when coupled with a scheduler

and runtime system, allows for many benefits, including higher performance and utilization of computational resources, easier programming and porting, and adaptations of code during runtime.

The system consists of a method of representing computer algorithms as a series of data-dependent tasks. The series forms a graph, which can be scheduled for execution on many nodes of a supercomputer efficiently by a computer algorithm. The schedule is executed by a dispatch component, which is tailored to understand all of the hardware types that

may be available within the system. The scheduler is informed by a cluster mapping tool, which generates a topology of available resources and their strengths and communication costs.

Software is decoupled from its hardware, which aids in porting to future architectures. A computer algorithm schedules all operations, which for systems of high complexity (i.e., most NASA codes), cannot be performed optimally by a human. The system aids in reducing repetitive code, such as communication code, and aids in the reduction of redundant code across projects.

It adds new features to code automatically, such as recovering from a lost node or the ability to modify the code while running.

In this project, the innovators at the time of this reporting intend to develop two distinct technologies that build upon

each other and both of which serve as building blocks for more efficient HPC usage. First is the scheduling and dynamic execution framework, and the second is scalable linear algebra libraries that are built directly on the former.

This work was done by John Humphrey and

Kyle Spagnoli of EM Photonics, Inc. for Goddard Space Flight Center. Further information is contained in a TSP (see page 1). GSC-16472-1

Σ Deepak Condenser Model (DeCoM)

Goddard Space Flight Center, Greenbelt, Maryland

Development of the DeCoM comes from the requirement of analyzing the performance of a condenser. A component of a loop heat pipe (LHP), the condenser, is interfaced with the radiator in order to reject heat. DeCoM simulates the condenser, with certain input parameters. Systems Improved Numerical Differencing Analyzer (SINDA), a thermal analysis software, calculates the adjoining component temperatures, based on the DeCoM parameters and interface temperatures to the radiator. Application of DeCoM is (at the time of this reporting) restricted to small-scale analysis, without the need for in-depth LHP

component integrations. To efficiently develop a model to simulate the LHP condenser, DeCoM was developed to meet this purpose with least complexity. DeCoM is a single-condenser, single-pass simulator for analyzing its behavior. The analysis is done based on the interactions between condenser fluid, the wall, and the interface between the wall and the radiator.

DeCoM is based on conservation of energy, two-phase equations, and flow equations. For two-phase, the Lockhart-Martinelli correlation has been used in order to calculate the convection value between fluid and wall. Software such as

SINDA (for thermal analysis analysis) and Thermal Desktop (for modeling) are required. DeCoM also includes the ability to implement a condenser into a thermal model with the capability of understanding the code process and being edited to user-specific needs. DeCoM requires no license, and is an open-source code. Advantages to DeCoM include time dependency, reliability, and the ability for the user to view the code process and edit to their needs.

This work was done by Deepak Patel of Goddard Space Flight Center. Further information is contained in a TSP (see page 1). GSC-16296-1

Σ Flight Software Math Library

Goddard Space Flight Center, Greenbelt, Maryland

The flight software (FSW) math library is a collection of reusable math components that provides typical math utilities required by spacecraft flight software. These utilities are intended to increase flight software quality reusability and maintainability by providing a set of consistent, well-documented, and tested math utilities. This library only has dependencies on ANSI C, so it is easily ported.

Prior to this library, each mission typically created its own math utilities using ideas/code from previous missions. Part of the reason for this is that math libraries can be written with different strategies in areas like error handling, parameters orders, naming conventions, etc. Changing the utilities for each mis-

sion introduces risks and costs. The obvious risks and costs are that the utilities must be coded and revalidated. The hidden risks and costs arise in miscommunication between engineers. These utilities must be understood by both the flight software engineers and other subsystem engineers (primarily guidance navigation and control).

The FSW math library is part of a larger goal to produce a library of reusable Guidance Navigation and Control (GN&C) FSW components. A GN&C FSW library cannot be created unless a standardized math basis is created. This library solves the standardization problem by defining a common feature set and establishing policies for the library's design. This allows the libraries

to be maintained with the same strategy used in its initial development, which supports a library of reusable GN&C FSW components.

The FSW math library is written for an embedded software environment in C. This places restrictions on the language features that can be used by the library. Another advantage of the FSW math library is that it can be used in the FSW as well as other environments like the GN&C analyst's simulators. This helps communication between the teams because they can use the same utilities with the same feature set and syntax.

This work was done by David McComas of Goddard Space Flight Center. Further information is contained in a TSP (see page 1). GSC-16102-1



Recirculating 1-K-Pot for Pulse-Tube Cryostats

A paper describes a 1-K-pot that works with a commercial pulse tube cooler for astrophysics instrumentation testbeds that require temperatures <1.7 K. Pumped liquid helium-4 cryostats were commonly used to achieve this temperature. However, liquid helium-4 cryostats are being replaced with cryostats using pulse tube coolers.

The closed-cycle 1K-pot system for the pulse tube cooler requires a heat exchanger on the pulse tube, a flow restriction, pump-out line, and pump system that recirculates helium-4. The heat exchanger precools and liquefies helium-4 gas at the 2.5 to 3.5 K pulse tube cold head.

This closed-cycle 1-K-pot system was designed to work with commercially available laboratory pulse tube coolers. It was built using common laboratory equipment such as stainless steel tubing and a mechanical pump. The system is self-contained and requires only common wall power to operate. The lift of 15 mW at 1.1 K and base temperature of 0.97 K are provided continuously. The system can be scaled to higher heat lifts of ≈ 30 to 50 mW if desired.

Ground-based telescopes could use this innovation to improve the efficiency of existing cryogenic systems or as a basis of new systems.

This work was done by Christopher G. Paine, Bret J. Naylor, and Thomas Prouve of Caltech for NASA's Jet Propulsion Laboratory. Further information is contained in a TSP (see page 1). NPO-48355

Method for Processing Lunar Regolith Using Microwaves

A paper describes a method of using microwave heating experiments on lunar simulants to determine the mechanism that causes lunar regolith to be such an excellent microwave absorber. The experiments initially compared the effects of sharp particle edges to round particle edges on the heating curves. For most compositions, sharp particle edged sam-

ples were more effective in being heated by microwaves than round particle edged materials. However, the experiments also showed an unexpected effect for both types of particles. Upon heating the sample surface above 400 °C, the sample experienced some sort of internal structure change that caused it to heat much more efficiently. This enhancement may be associated with the unique microwave volumetric heating that can produce a large temperature gradient within the sample leading to melting of some components at the center of the sample. This new effect that may also be happening in lunar regolith samples is probably the cause of the previously observed enhanced heating of a sample of lunar regolith. Properly designed microwave applicators could heat and solidify the lunar regolith to form roads and building blocks for structures needed on the Moon.

This work was done by Martin B. Barmatz and David E. Steinfeld of Caltech for NASA's Jet Propulsion Laboratory. Further information is contained in a TSP (see page 1). NPO-48895.

Wells for *In Situ* Extraction of Volatiles from Regolith (WIEVR)

A document discusses WIEVRs, a means to extract water ice more efficiently than previous approaches. This water may exist in subsurface deposits on the Moon, in many NEOs (Near-Earth Objects), and on Mars. The WIEVR approach utilizes heat from the Sun to vaporize subsurface ice; the water (or other volatile) vapor is transported to a surface collection vessel where it is condensed (and collected). The method does not involve mining and extracting regolith before removing the frozen volatiles, so it uses less energy and is less costly than approaches that require mining of regolith.

The only drilling required for establishing the WIEVR collection/recovery system is a well-bore drill hole. In its simplest form, the WIEVRs will function without pumps, compressors, or other gas-moving equipment, relying instead on diffusive transport and thermally induced convec-

tion of the vaporized volatiles for transport to the collection location(s). These volatile extraction wells could represent a significant advance in extraction efficiency for recovery of frozen volatiles in subsurface deposits on the Moon, Mars, or other extraterrestrial bodies.

This work was done by Otis R. Walton of Grainflow Dynamics Inc. for Glenn Research Center. Further information is contained in a TSP (see page 1).

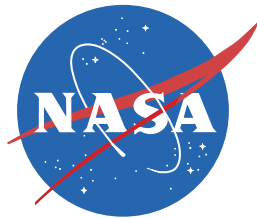
Inquiries concerning rights for the commercial use of this invention should be addressed to NASA Glenn Research Center, Innovative Partnerships Office, Attn: Steven Fedor, Mail Stop 4-8, 21000 Brookpark Road, Cleveland, Ohio 44135. Refer to LEW-19017-1.

Estimating the Backup Reaction Wheel Orientation Using Reaction Wheel Spin Rates Flight Telemetry from a Spacecraft

A report describes a model that estimates the orientation of the backup reaction wheel using the reaction wheel spin rates telemetry from a spacecraft. Attitude control via the reaction wheel assembly (RWA) onboard a spacecraft uses three reaction wheels (one wheel per axis) and a backup to accommodate any wheel degradation throughout the course of the mission. The spacecraft dynamics prediction depends upon the correct knowledge of the reaction wheel orientations. Thus, it is vital to determine the actual orientation of the reaction wheels such that the correct spacecraft dynamics can be predicted.

The conservation of angular momentum is used to estimate the orientation of the backup reaction wheel from the prime and backup reaction wheel spin rates data. The method is applied in estimating the orientation of the backup wheel onboard the Cassini spacecraft. The flight telemetry from the March 2011 prime and backup RWA swap activity on Cassini is used to obtain the best estimate for the backup reaction wheel orientation.

This work was done by Farheen Rizvi of Caltech for NASA's Jet Propulsion Laboratory. Further information is contained in a TSP (see page 1). NPO-48350



National Aeronautics and
Space Administration